SANDIA REPORT

SAND2001-2227
Unlimited Release
Printed July 2001

Characterization of the Air Source and the Plume Source at FLAME

Thomas K. Blanchat

Prepared by
Sandia National Laboratories
Albuquerque, New Mexico 87185 and Livermore, California 94550

Sandia is a multiprogram laboratory operated by Sandia Corporation, a Lockheed Martin Company, for the United States Department of Energy under Contract DE-AC04-94AL85000.

Sandia National Laboratories

Issued by Sandia National Laboratories, operated for the United States Department of Energy by Sandia Corporation.

Available to DOE and DOE contractors from
U.S. Department of Energy
Office of Scientific and Technical Information
P.O. Box 62
Oak Ridge, TN 37831

Telephone: (865)576-8401
Facsimile: (865)576-5728
E-Mail: reports@adonis.osti.gov
Online ordering: http://www.doe.gov/bridge

Available to the public from
U.S. Department of Commerce
National Technical Information Service
5285 Port Royal Rd
Springfield, VA 22161

Telephone: (800)553-6847
Facsimile: (703)605-6900
E-Mail: orders@ntis.fedworld.gov
Online order: http://www.ntis.gov/ordering.htm

SAND2001-2227
Unlimited Release
Printed July 2001

Characterization of the Air Source and the Plume Source at FLAME

Thomas K. Blanchat
Nuclear Safety Testing Department
Sandia National Laboratories
P.O. Box 5800
Albuquerque, NM 87185-1139

ABSTRACT

This report describes the characterization of the air source and the plume source at FLAME (the Fire Laboratory for Accreditation of Models by Experimentation). FLAME was designed to perform large indoor fire validation experiments and similar engineering sciences research activities. Validation experiments are a special class of experiment in that they are specifically designed for direct comparison with the computational models. Making meaningful comparison between the computational and experimental results requires careful characterization and control of the experimental features or parameters used as inputs into the computational model. Validation experiments must be designed to capture the essential physical phenomena, including all relevant initial and boundary conditions.

To that end (controlling and characterizing FLAME boundary conditions), functions have been developed to control the blowers as a ganged unit at desired flow rates. A function has been developed to yield the desired air source average velocity at a chosen blower flow rate. The diffuser source was shown to be very uniform across the planar exit. Velocity characterization date (average velocity, standard deviation, and standard error) were determined for the ducts, the air source, and the diffuser source.

This page intentionally left blank

CONTENTS

FIGURES

Page

FIGURES (continued)

Page

TABLES

This page intentionally left blank

ACKNOWLEDGEMENTS

The author is grateful to and cheerfully acknowledges the following personnel who had major roles in this undertaking. Sheldon Tieszen and Tim O'Hern recognized the need to characterize the facility boundary conditions. T.Y. Chu provided the inspiration and the resources. Chuck Hanks, Pat Drosda, John Garcia, and Rod Oliver sweated the instrumentation, calibration, and mechanical details. This report is proof of their expertise in experiment setup and performance.

This work was supported by the United States Department of Energy and was performed at Sandia National Laboratories. Sandia is a multiprogram laboratory operated by Sandia Corporation, a Lockheed Martin Company, for the United States Department of Energy under Contract No. DE-AC04-94AL85000.

This page intentionally left blank

INTRODUCTION

The Fire Laboratory for the Accreditation of Models and Experiments (FLAME) is being used to acquire data sets for buoyant, non-reacting and reacting flows of sufficient quality to support validation of numerical simulation tools. To achieve this goal, not only must simultaneous temporal and spatial imaging with sufficient resolution be obtained for the flow of interest, but the geometry, initial conditions, and boundary conditions must also be specifiable with sufficient resolution.

This report describes boundary condition measurements taken to characterize the air source and the plume source at FLAME. The purpose is twofold. First, to provide the analysts with a reasonable set of measurements for the current series of experiments utilizing particle image velocimetry (PIV) for velocity field measurements and planar laser induced fluorescence (PLIF) for scalar field measurements. Second, to provide the operators and experiments of FLAME with a knowledge database to allow controlling the boundary conditions with some repeatability.

This page intentionally left blank

FLAME BUILDING

Figure 1 shows the Fire Laboratory for Accreditation of Models and Experiments (FLAME) facility. Overall, the facility contains a central chamber containing the experimental apparatus, a long chimney centered over the central chamber, and external hardware to supply air to the central chamber and cooling water to the walls. Extensive internal structures exist for air and plume gas sources, with an external high-pressure gas delivery system for the plume source.

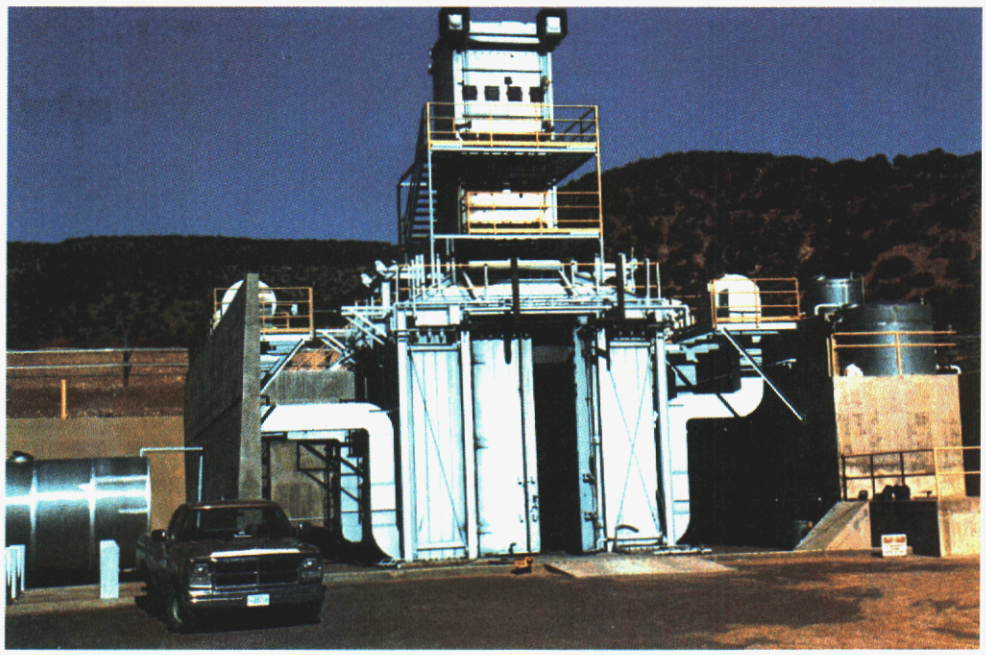

Figure 1. The Fire Laboratory for Accreditation of Models and Experiments (FLAME). (Note ducting from the four blowers to the base of FLAME).

The following descriptions of the building and experimental apparatus used in the PIV/PLIF experiments were taken from *Spatial and Temporal Resolution of Fluid Flows* (Tieszen et al. 1998). Figure 2 shows that the central chamber is a nominally 6.1-m (20 ft) cube. The floor of the facility is 2.45 m below the plume source. The floor is flat with a subfloor in the center of the chamber 0.51 m below the main floor. The subfloor is 3.05 m on a side and is centered under the chimney. The bottom and four sides for the FLAME facility are enclosed except for four air inlets into the lower four corners of the facility. The ceiling is not horizontal but tapers upward toward the opening to the chimney at the center of the facility. The ceiling taper is 32 degrees (from the horizontal) beginning at 3.55 m above the plume source and ends at the opening to the chimney. The chimney opening is at an elevation of 4.56 m above the plume source. The chimney is square in cross section, nominally 2.3 m (7.5 ft) on each side, and extends an additional 7.32 m (24 ft) above the central chamber.

The facility is made principally of 0.305-m wide by 0.102-m deep (12 in by 4 in) channel with a nominal 4.75-mm (3/16 in) wall thickness. The channels are interconnected to allow a cooling fluid (glycol/water mix) to be pumped through the walls to cool them. Because of the short

duration of the fires in this PIV/PLIF experimental program, the channel cooling was not required. The ceiling and a 1.2-m high segment of the sidewalls where it joins the ceiling are protected with a 1.6 mm thick stainless steel radiation shield. These shields are mounted with a 10-cm offset into the facility to provide thermal protection for large, long duration fires. An outer structure of steel beams is used to provide additional structural reinforcement to permit a small internal explosion without damage to the facility. Access to the facility is through two large doors, 1.52 m (5 ft) wide by 5.49 m (18 ft) high, located in the center of the south wall.

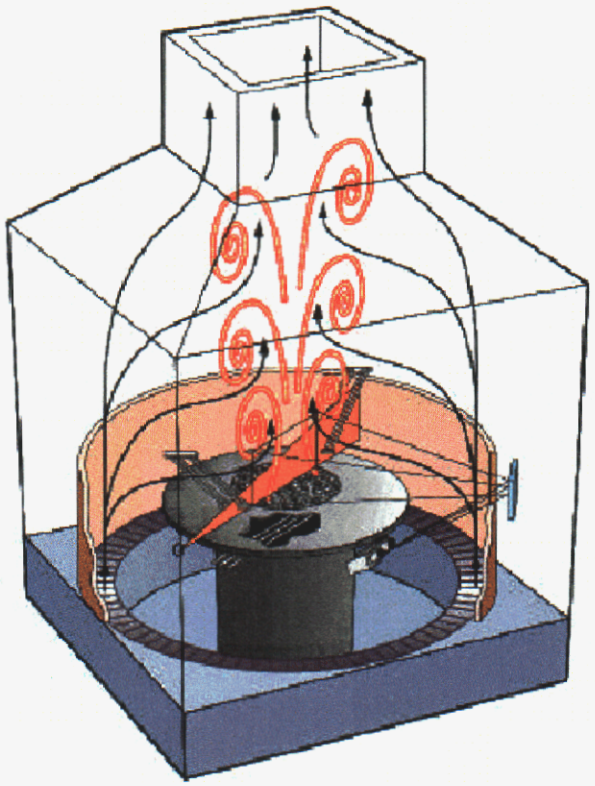

Figure 2. Illustration of the air source and plume source in FLAME.

Figure 2 shows that during normal operation, the access doors are closed and the only inlets to the facility are from the plume and ambient air sources; the only exhaust (with the exception of negligible leaks) is through the chimney. The hardware associated with each of these sources will be discussed separately in the following sections.

Plume Source

The plume source for these experiments is shown in Figure 3. The diameter of the source is nominally 1 m and is surrounded by a 0.51-m wide sheet steel lip, which represents the ground plane. The centerline of plume is coaxially located with the center of the central chamber and the chimney to within approximately 5 cm. The center of the plume at its surface is the location of the coordinate system origin, $(r,\theta,z) = (0, 90°, 0)$.

In the initial PIV/PLIF experiments, the material at the surface of the plume source was a 2.54-cm thick porous ceramic plate with nominal pore size of 2.5 mm (10 pores per inch). Later

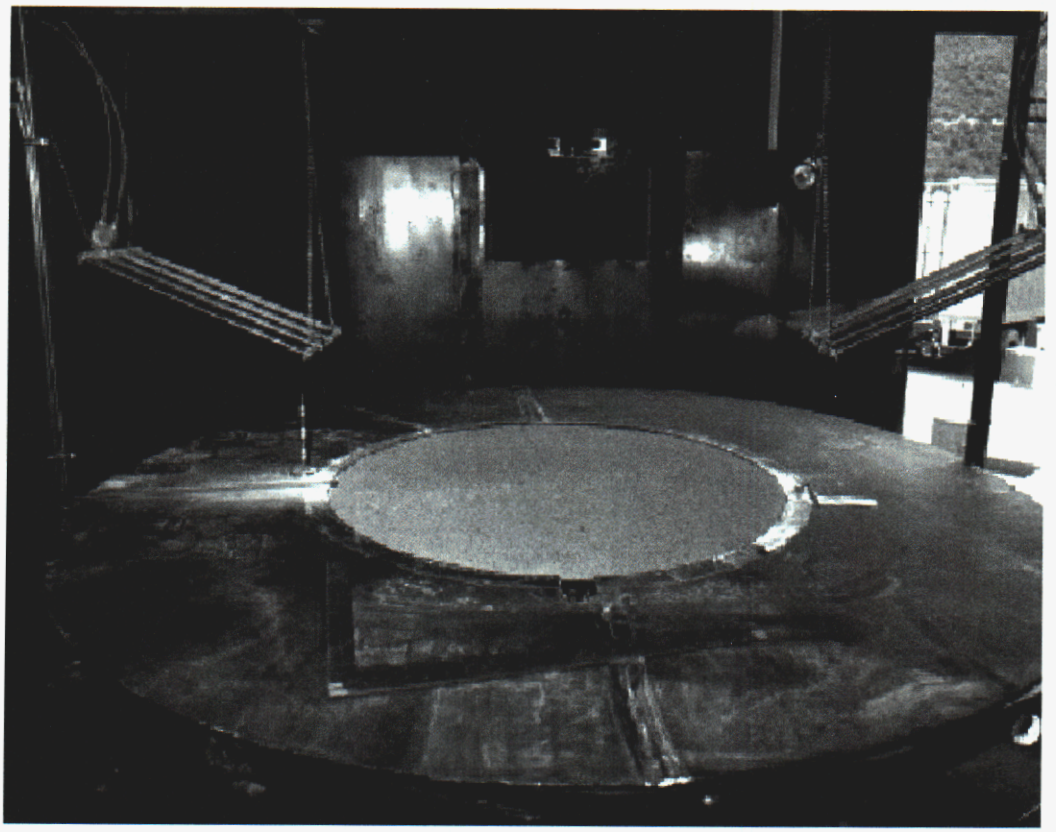

Figure 3. Plume Source

experiments used a metal honeycomb, constructed from 304 stainless steel 0.004-inch thick. The honeycomb (1/8-inch hexagonal cells) plate was 1-inch tall. The percent open area of the honeycomb was estimated to be 92%. The characterization of the diffuser ground plane surface was performed over this metal honeycomb material.

The surface of the ground plane surrounding the plume source is made of 4-mm plate steel and is uniform to within about 6 mm. The ground plane is supported on a 2.9-cm thick steel grating backup held on unistrut supports which carry the weight into a welded steel frame used for support. With the exception of one square cutout, the surface of the ground plane is continuous with aluminized tape to seal joints within the lip, and between the lip and the plume. The square cutout is located at the edge of the plume source at an angle of 270°. The hole is 0.05 m circumferentially by 0.09 m radially and permits access to the plume for an ignitor system mounted under the ground plane.

The plume source rests upon a large diffuser that is part of the gas flow system for the plume. The diffuser shown in Figure 4 is approximately 3-meters tall and extends down 0.51 m below the main floor of the facility to a subfloor at the center of the chamber. The diffuser is nominally 1.0 m in diameter for 1 m below the plume source. A pressure relief vent in the waist of the diffuser increases its diameter to 1.2 m for 0.27 m. Below the relief valve, the diffuser has a diameter of 0.95 m to the floor level. Below floor level, it has a hemispherical lower head. The material in the upper part of the diffuser is 3-mm thick steel sheet stock while in the lower part it is 18-mm thick stainless steel. Note that ring air source is visible in the foreground of Figure 4.

Figure 4. Plume source plane and diffuser.

The gas composition of the plume is created from two independent gas lines leading from compressed gas bottle farms. Each line is supplied by six or twelve 43.8-liter compressed gas cylinders each containing nominally 7.7 m^3 of gas at local ambient conditions. The two high-pressure flows are regulated to intermediate pressure, measured, choked to produce independence, mixed, and then diffused to produce a low velocity (less than one meter per second) flow across a one-meter source.

High-pressure gases flow into the manifold from the bottle farms at a maximum of 14 MPa. The lines are valved so that the "diluent" side can flow into the "fuel" side to allow purging of the system when combustible gases are used, although the two lines normally flow independently during a test. The flows are passed through filters to remove dust from gas bottle storage and then the pressure is dropped to nominally 1.4 MPa by high-flow-rate (Circle Seal SR800) pressure regulators. As with all gas systems, manual and pressure relief valves are present for safety purposes. The pressure, temperature, and flow rate of the gas in each line are measured. High and low range flowmeters are used to ensure accuracy across a broad range of flows. The flow in each line then passes through a flow controller valve (Jordan Mk 708). These valves are run under choked conditions such that the upstream flow is independent of the downstream flow. Downstream of the flow controller valves, the two gas streams are merged into a single gas stream in a 5-cm diameter pipe. Running the flow controller valves in a choked state decouples the pressure regulators from turbulent mixing instabilities as the lines merge, thus preventing

'dueling regulators.' Mixing of the flows occurs in the 5-cm diameter pipe which runs through nominally 4.5 m and three 90° elbows before being dumped into the diffuser.

The final element within the primary gas flow system is the diffuser. The flow exiting the top of the diffuser is the plume source. The gas enters the base of the diffuser through the 5-cm tube in the center of, and aligned coaxially with, the diffuser. Depending on the flow rates, the pressure in the 5-cm tube may be sufficiently high to choke at its exit into the 0.91-m internal diameter of the lower part of the diffuser. In any case, the diffuser area is so large that the pressure in the diffuser is nearly ambient. The resulting jet flow into the lower portion diffuser is broadened out by a series of four plates with decreasing hole diameters (2.5 cm, 1.9 cm, 1.3 cm, and 0.95 cm) but relatively fixed blockage ratio of approximately 0.5. The plates and spacing between them is taken from a proven diffuser design used in Sandia's wind tunnels. Each of the plates is backed up by grating to provide support for the drag loads placed on the plates by the diverging jet. The final plate is backed up by 10-cm thick grating. It is bolted into the diffuser with spring-loaded bolts such that if the plate becomes plugged (for any reason), the pressure in the lower part of the diffuser will vent at 0.2 MPa. Above the lower diffuser head, the diffuser broadens from 0.91 m to 1.00 m via a short 5-cm taper. To resettle the flow after the expansion, two 24 by 24 mesh screens with 0.25-mm wire diameter (57.9% open area) are used, one immediately following the expansion and the second 2 cm downstream. Two layers of 2.54-cm thick stainless steel honeycomb directly over a 5.08-cm thick aluminum honeycomb are used to reduce the turbulence in the flow. The honeycomb has a nominal cell size of 3 mm. The top of the honeycomb defines the diffuser exit plane.

Air Source

Numerical simulation of the flow patterns within the FLAME facility was used to design the manner in which air was distributed in the facility. To achieve the desired radial inflow, it was necessary to introduce the air symmetrically into the facility. Since air enters the walls at only four 0.61-m square openings at the base of the east and west walls in the north and south corners, substantial ductwork had to be created. In the resultant design, the duct work channels the air so that it enters the central chamber with only a vertical velocity component from an annular surface with an inner radius of 2.30 m and an outer radius of 2.91 m. The top surface of the air source is located 1.74 m below the ground plane, 0.71 m above the facility floor. The annulus is fabricated from sixteen 45° segments, four to each quadrant of the facility. The segments are not rounded but flat on each side so as to be easy to fabricate and yet adequately approximate an annulus.

While the facility can be operated in a free draw mode, four fans (Dayton No. 3C109 with 5 HP motor) with a maximum capacity of 4.7 m^3/sec (10,000 scfm) each can also supply air to the facility. The surface area of the annular air source is 9.66 m^2, resulting in a maximum velocity of about 1.9 m/s. The fans are infinitely variable between zero and their maximum value so that the air inlet velocity can be adjusted.

The numerical simulations indicated that as long as the flow rate from the air ducts is less than a critical value for a given plume flow, a trapped vortex will form beneath the ground plane. The vortex will stay trapped below the plane of the plume and radial inflow into the plume will result. If the airflow rate is too high, the top of the trapped vortex will climb above the plane of the

plume and a region of downflow will occur along the plume. This downflow results in a fairly complex flow pattern in which counterflow exists along the sides of the plume except at its base where the solid lip forces radial inflow at the base. Hence, the flow rate of the air needs to be adjusted below a set value for each plume flow in order for radial inflow to result in the facility.

The numerical simulations also showed that the air velocities were sufficiently high at the surface of the air ducts that radial inflow was not possible in the square FLAME facility without providing overall radial symmetry to an elevation just above the surface of the burner. Therefore, sixteen 0.61-mm thick, 3.05-m tall, steel sheets were hung vertically on unistrut frames such that they provided the cylindrical shield wall shown (cutaway) in Figure 2. These sheets prevent corner flows from disrupting the radial symmetry. The bases of the sheets begin in the air ducts 0.30 m above the floor (an elevation of -2.15 m) and run to an elevation of 0.90 m. The sheets can be seen in the background in Figure 3.

To facilitate air flow from the air inlets in the four corners of the FLAME facility to the annular air vent, the entire area between the cylindrical shield wall and square FLAME facility walls has been turned into an air duct. Essentially, a false floor has been created 0.79 m above the facility floor (1.61 m below the ground plane). Baffles are used to channel the air between the false floor and the facility floor from the four corners into the annular vents. Six baffles are used in each quadrant, four to the vertices of the four segments making up the annulus and two additional baffles to subdivide the middle segments.

In a manner similar to the gas plume diffuser, the air ducts have horizontally mounted plates and screens to create a uniform flow exiting the top of the ducts. Two plates, two screens, and a honeycomb are used. The lowest plate is mounted above the lower edge of the shield wall, at 0.51 m above the floor. In 5-cm increments, the next plate, two screens and the 0.5-cm high honeycomb are mounted. The plates have a fixed blockage ratio of approximately 0.5; with the lower one having 2.5-cm holes and the upper one having 1.3-cm holes. The screens are 24 by 24 mesh with a 0.25-mm wire diameter yielding a 57.9% open area. The aluminum honeycomb has 3-mm cells.

Chimney Exhaust

The only outlet of the facility is through the chimney. The square chimney has insulation mats on the inside faces and remains nominally 2.3 m on each side throughout its height except at the exit. The chimney height is nominally 7.32 m. At the exit, the north and south faces taper inward at nominally 45-degree angles to leave a 1.2-m (4 ft) by 2.4-m (8 ft) opening at the exit. Nominal 1.2-m (4 ft) long by 2.4-m (8-ft) doors, hinged on the east and west side, open outward at nominally 135 degrees from the exit plane during a test. The chimney is deliberately obstructed by pipes throughout its length. The pipes induce mixing in the duct channel while the flow is still hot. The additional mixing partially oxidizes the soot (smoke) from the fire in the central chamber. Because of the pipes, the chimney is not as efficient as it could be in drafting. However, the pipes provide some buffering between the central chamber and the exit, so that slight changes in air pressure at the exit due to light breezes are not directly felt within the central chamber.

BLOWER AND DUCTWORK CHARACTERIZATION AT FLAME

Introduction

Characterization of the four blowers and associated ductworks at FLAME was a necessary first step for the upcoming large-scale PIV flame plume experiments. A calibration curve (average duct volumetric flow rate as a function of the installed Kurz anemometer voltage) for each blower was necessary to allow accurate setting and matching of the airflow in the air exhaust ring over the four quadrants.

Procedure

A 16-point scan using a TSI hot-wire anemometer (Model 8455) was performed on each blower duct at FLAME. The TSI Air Velocity Transducer Model 8455 is NIST traceable and includes a calibration certificate. The TSI hot-wire probe specifications include:

1. Minimum Accuracy is ±2.0% of reading or ±0.5% of full scale of selected range
2. Repeatability <±1.0% of reading (based on one minute average from 0.5 to 5.0 m/s)
3. Response Time to Flow is 0.2 sec (for 63% of final value, tested at 7.5 m/s)
4. Field Selectable Velocity Ranges (0.125 m/s to 1.0, 1.25, 1.50, 2.0, 2.5, 4.0, 5.0, 7.5, 10.0, 12.5, 5.0, 10.0, 25.0, 30.0, 40.0, 50.0 m/s)
5. Minimum Resolution is 0.07% of selected full scale
6. Output Time Constant (field selectable) ranges from 0.05 to 10 seconds
7. Temperature Compensation Range:0 to 60°C, Sensor and Electronics Operation and Storage: 0 to 93°C.

Figure 5 shows the spatial locations where velocity was measured in each of the four inlet ducts. The PID controller for each blower was first set to 1 volt and, after the flow stabilized, the TSI scan commenced. A data point consisted of manually inserting the TSI probe to the selected position, waiting about 15 s for the measurement to stabilize, and then recording data (at 1 sample/s) for the next 15 s. The recorded velocity data for each blower is listed in Tables A1, A3, A5, and A7 in Appendix A for each blower. The scan was repeated at PID controller settings of 2, 3, 4, and 5 volts.

Results

Tables A2, A4, A6, and A8 (Appendix A) give the average and standard deviation of the duct velocity (in standard m/s) and the duct flow rate (in SCFM) as a function of the installed 4-probe Kurz hot-wire anemometer voltage. A linear average was performed since each scan area was uniform (6 by 6 inch square). Flow rate was determined by multiplying the average duct velocity by the duct area (24 by 24 inch square).

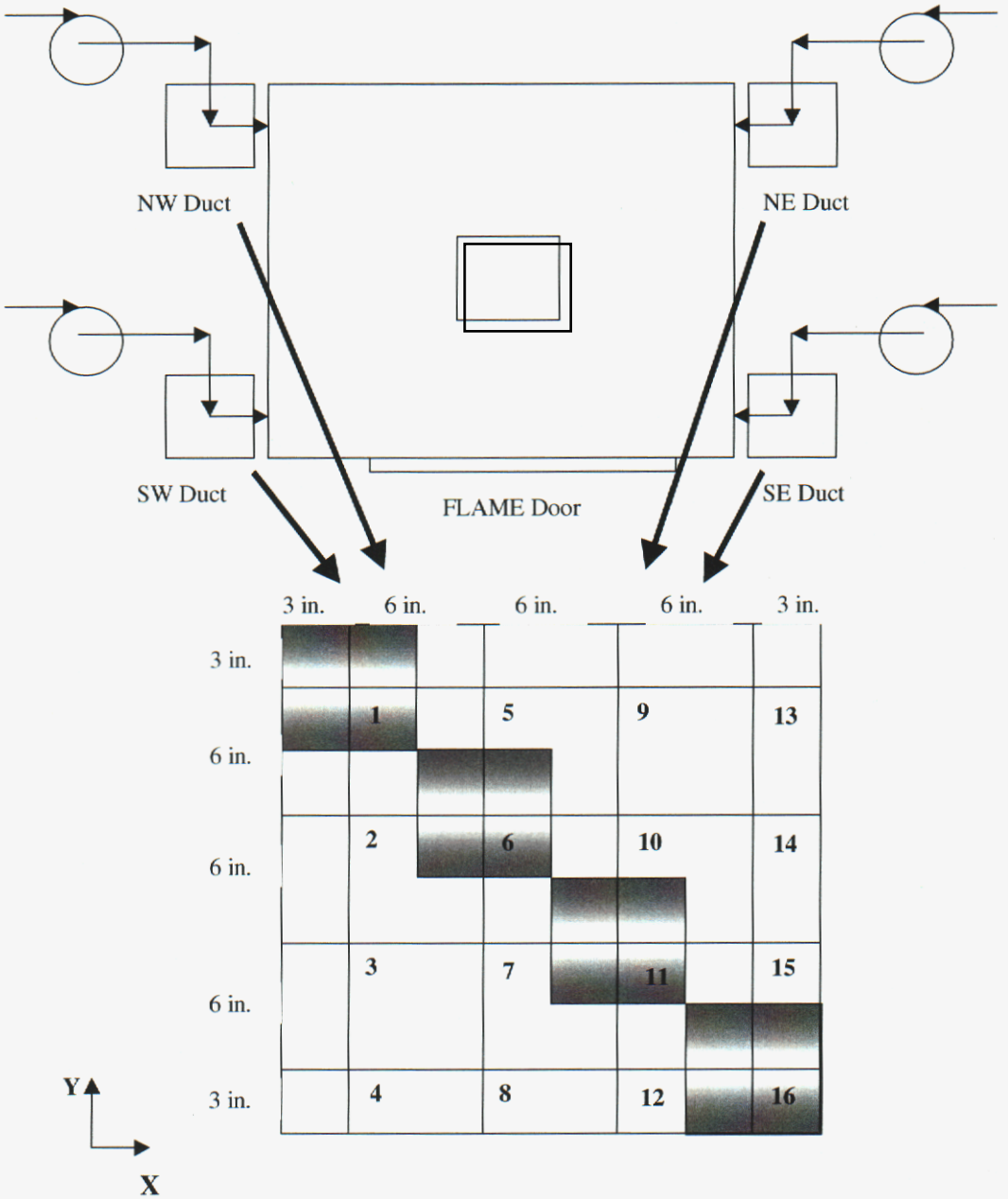

Figure 5. Blower Duct Scan Layout – 16 points – Equal Area (6 x 6 inch squares)

Figure 6 presents the carpet plots of spatial velocity at the five PID controller voltages for each duct. The velocity standard error (standard deviation/average) was about 5% for each speed and each blower. Figure 7 presents the volumetric flow rate as a function of the voltage measured by the permanently installed Kurz anemometer for each blower and associated duct. The first-order regression fit parameters are given in Table 1. These fit parameters have been installed in the LabView© blower operation program at FLAME, enabling accurate and stable flow rates from each blower.

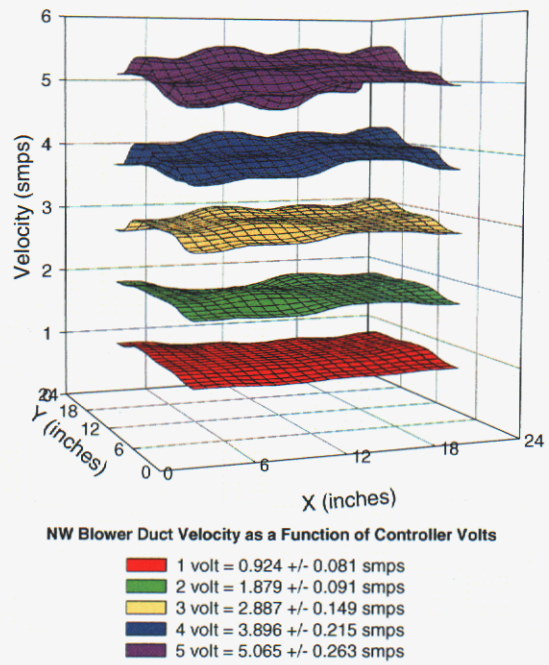

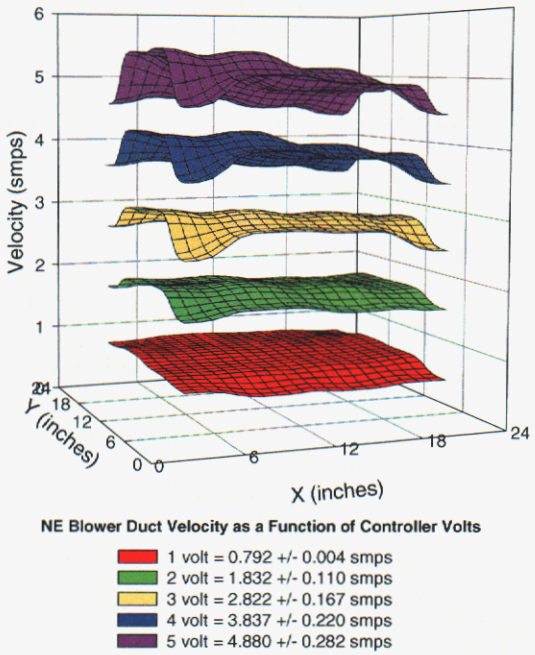

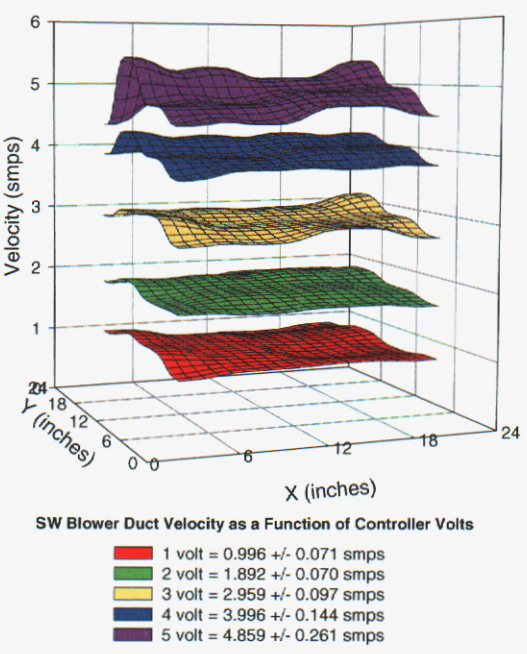

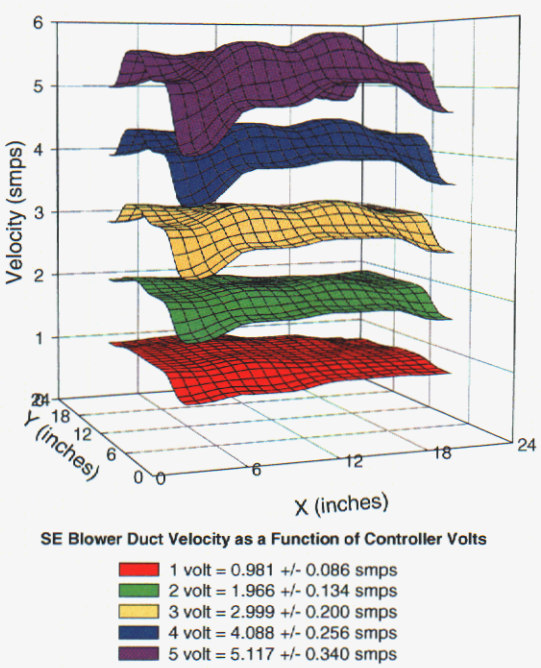

Figure 6. Velocity profiles in each duct at five blower speeds.

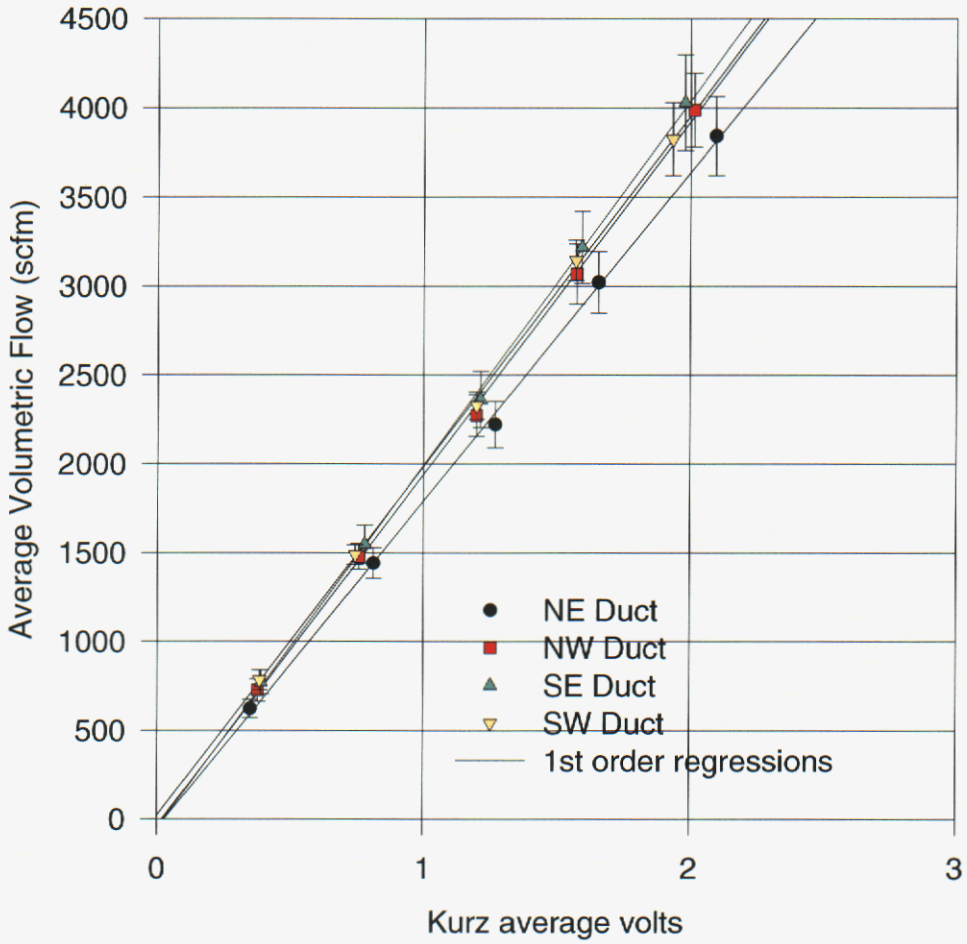

Figure 7. Duct volumetric flow rate as a function of the installed Kurz anemometer.

Table 1. Blower regression fit parameters.

parameter	NE	NW	SE	SW
b[0]	-50.2852	-37.4521	-50.8635	20.0094
b[1]	1844.2864	1980.6333	2046.2006	1968.0061
r^2	0.9989	0.9990	0.9989	0.9993

SCOPING MEASUREMENTS ON THE AIR INLET RING

Introduction

Characterization of the air source, or air inlet ring, flow at FLAME is necessary for previous and upcoming large-scale PIV flame and plume experiments in order to provide boundary conditions to code modelers. Scoping measurements were made on the air inlet ring to determine the data and methodology required to fully characterize the flow field.

Procedure And Results

Figure 8 gives a plan of the air inlet ring layout at FLAME. Eleven traverses were performed on the #2 segment or panel (SW quadrant) using a TSI hot-wire anemometer (Model 8455). Table 2 indicates that the blower speed (a function of PID controller voltage) and the probe height above the honeycomb were varied between traverses. Figure 9 shows that each traverse consisted of eleven measurements (3 inches apart) starting from the back wall of the ring to the segment front (the last two measurements were past the ring).

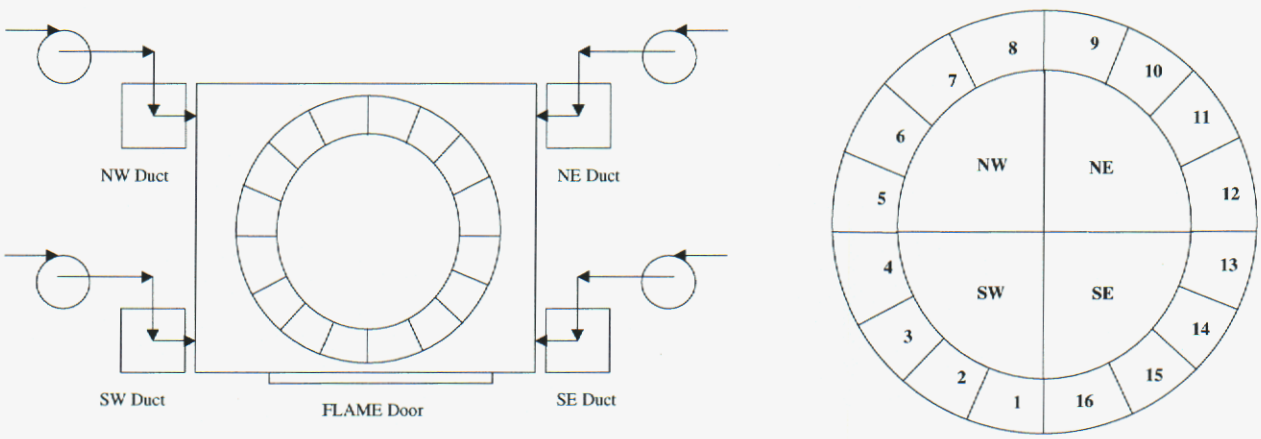

Figure 8. Air Inlet Ring Layout (4 quadrants, 16 panels)

Table 2. Parameters for the Eleven Traverses of Ring Segment #2.

Height Above Ring Segment (inches)	**Run Number**				
1	1	2	3	4	5
2	6		7		8
4	9		10		11
Blower Volts	**1**	**2**	**3**	**4**	**5**

The front door to FLAME was closed and the chimney vents were fully opened. The first traverse started with all blower PID controllers set to 1 volt and, after the flow stabilized, the TSI scan commenced. A data point consisted of moving the TSI probe to the selected position, waiting about 15 s for the measurement to stabilize, and then recording data (at 1 sample/s) for the next 15 s. The scan was repeated at PID controller settings of 2, 3, 4, and 5 volts.

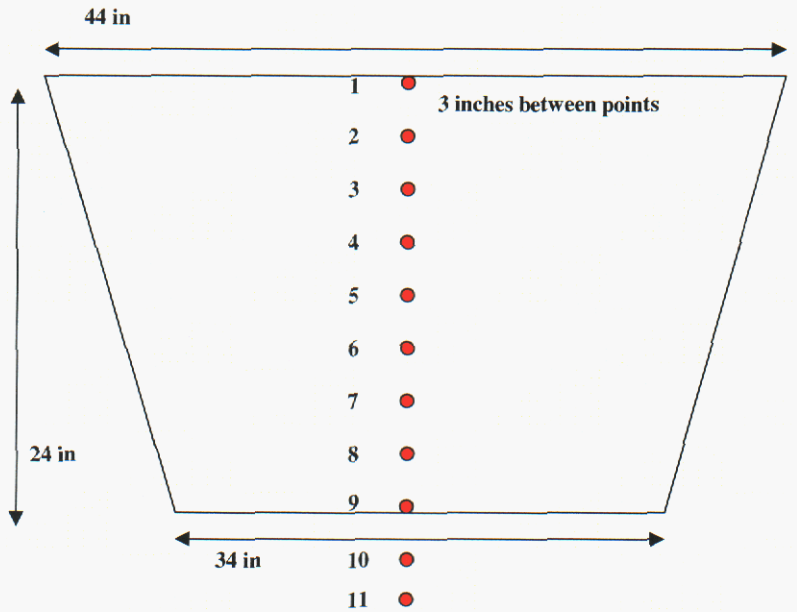

Figure 9. The TSI hot-wire traverse measurements across segment #2.

Figure 10 shows air velocity above the ring segment is shown as a function of position and blower speed. Figure 11 gives the flow rate from the SW blower, determined from the previously determined fit of the Kurz anemometer. The velocity was fairly uniform across the panel segment and appeared to be relatively unaffected by the variation in height. Note that a measurable air speed was found outside the direct path of the segment (the direction of flow was not determined).

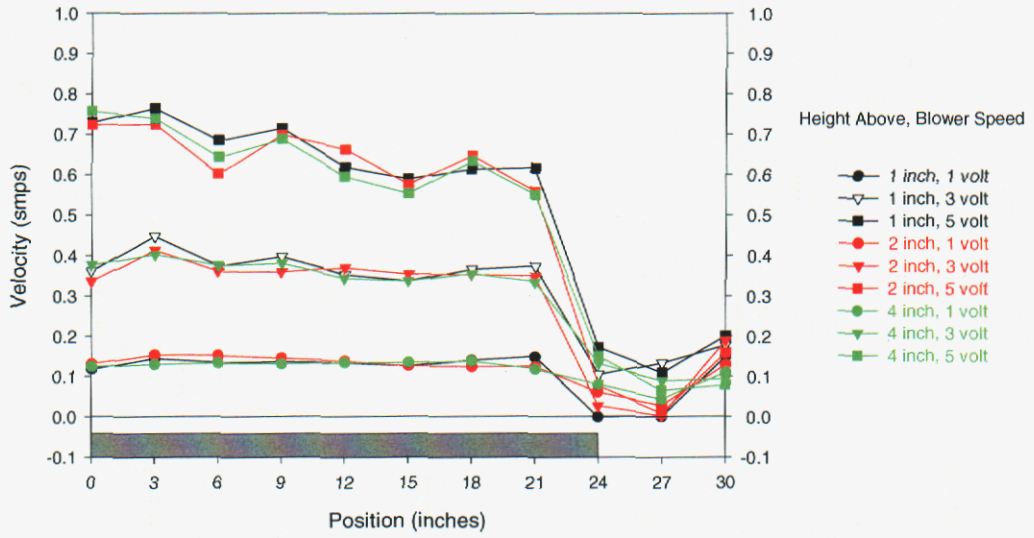

Figure 10. Velocity Profile above ring segment #2 as a function of height and blower speed.

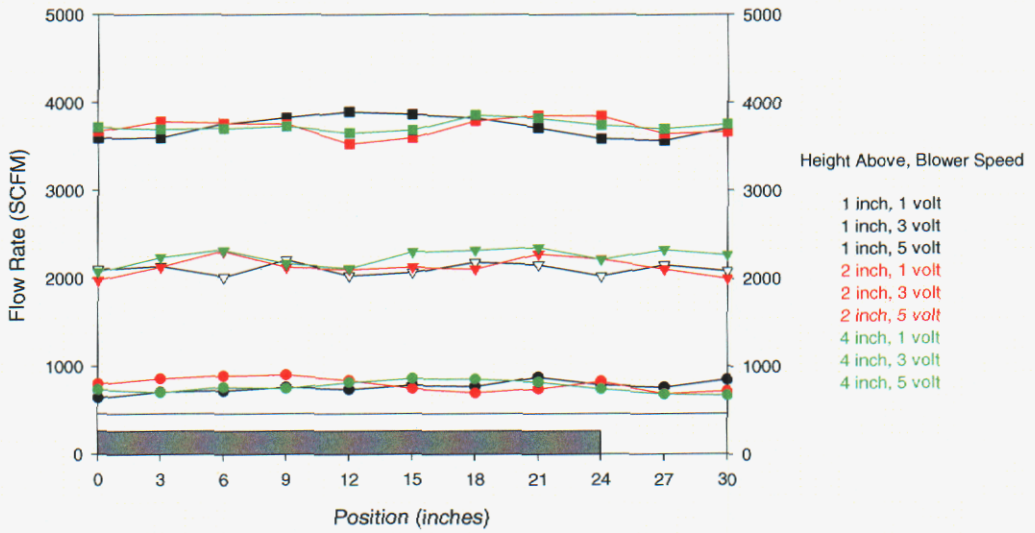

Figure 11. Blower flow rate during the ring segment #2 traverses.

The SW average *duct velocity* was previously found to be about 1.0, 3.0. and 4.9 m/s (standard) for a PID controller voltage of 1, 3, and 5 volts, respectively. Simple ratios (duct area / 4 x panel area) suggest that the *panel exhaust velocity* would be about 0.15, 0.46, and 0.75 m/s at the three blower settings. This was close to the measured values.

A quick scoping measurement of velocity uniformity between all panels was desired. To that end, a flow concentrator was fabricated using sheet metal (see Figure 12).

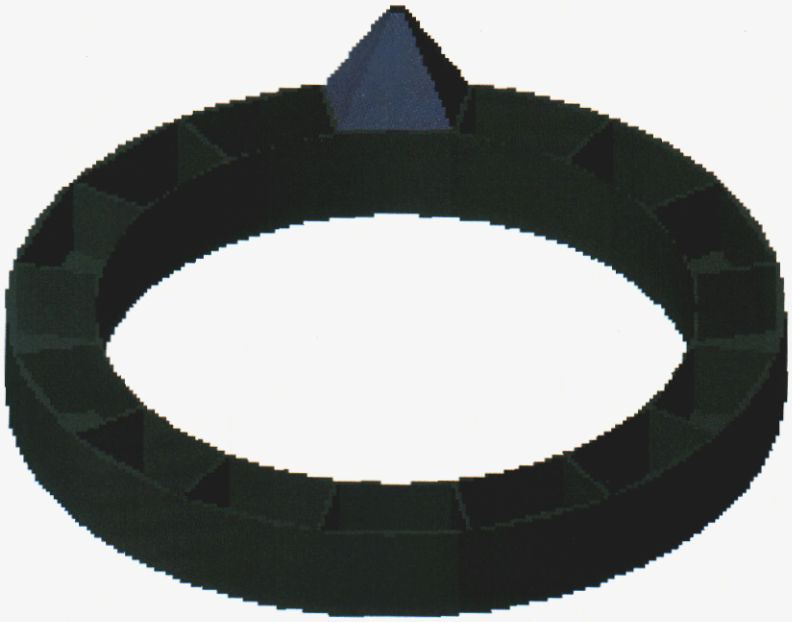

Figure 12. The flow concentrator over a ring segment.

The concentrator or cone was three feet tall. The inlet of the flow concentrator had the same dimensions as a ring segment panel, yielding an inlet area of 936 in^2. The concentrator outlet was a centered 4 by 4-inch square. The inlet to outlet area ratio was 58.5. The blower program at FLAME was modified to allow setting and controlling all blowers to a selected flow rate. The air velocity at the concentrator exit was measured at 14 ring panels with all blower controllers set at 600, 1000, 2000, and 4000 SCFM. Two ring panels could not be measure due to a physical interference. Table 3 presents the mean and standard deviation of the four blower flow rates and the cone exit velocity.

Table 3. Results of the Cone Concentrator Test.

Blowers Flow rate Mean ± Std.Dev. (scfm)				
	600	**1000**	**2000**	**4000**
NE	615.0 ± 22.5	998.4 ± 9.6	2010.3 ± 16.2	3524.7 ± 25.6
SE	609.1 ± 20.0	993.7 ± 8.9	2003.7 ± 60.7	3803.3 ± 9.1
NW	601.1 ± 27.5	1006.1 ± 6.9	2018.7 ± 17.8	3818.8 ± 99.6
SW	608.2 ± 17.0	998.6 ± 11.9	2015.6 ± 15.7	3636.3 ± 54.4
Cone Concentrator Velocity Mean ± Std.Dev. (smps)				
	0.97 ± 0.05	1.43 ± 0.04	2.50 ± 0.09	4.31 ± 0.16

Figure 13 shows the cone exit velocity measurements. The velocity was remarkably uniform; the standard error (standard deviation/average) of the velocity of all panels was within 3-5%. Figure 14 shows that the blower control was very stable and uniform at all speeds up to 2000

SCFM (the low flow rate and larger deviations at 4000 SCFM were caused by the PID controllers and were subsequently fixed by increasing the proportional band).

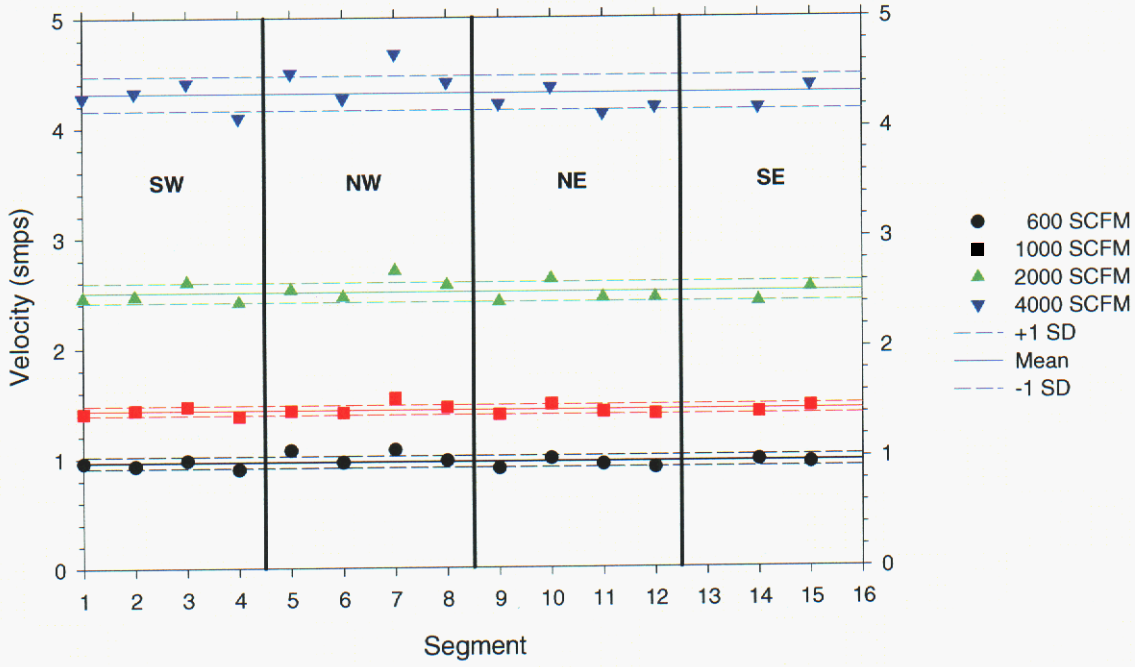

Figure 13. Velocity (mean and standard deviation) of 14 panels using the cone concentrator.

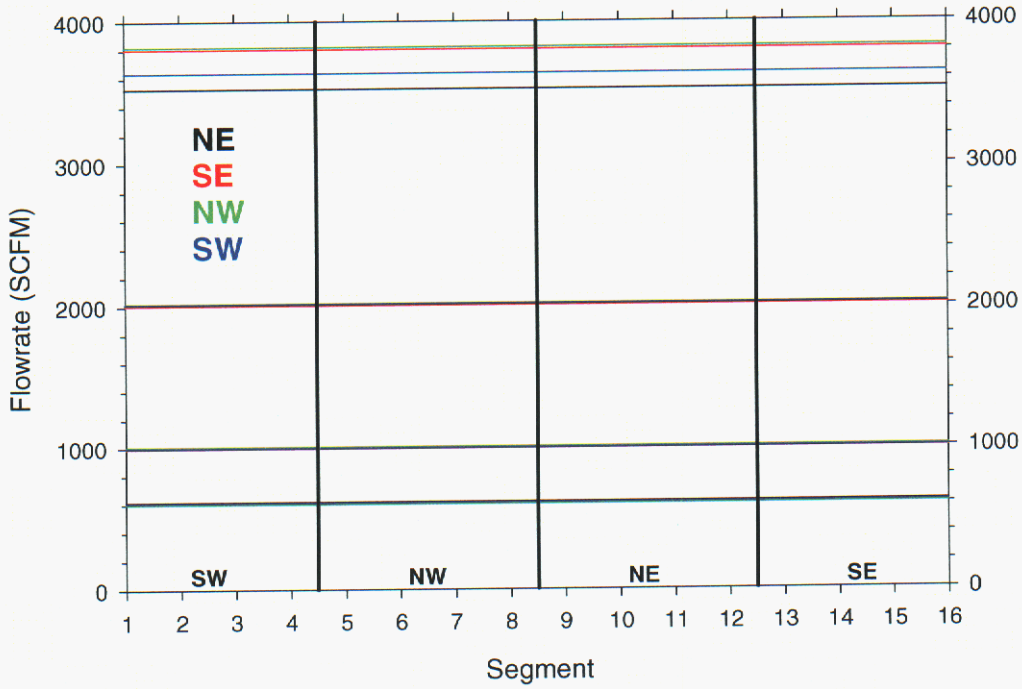

Figure 14. Blower flow rates during the cone test.

Conclusions

The blowers can now be ganged to yield identical flow rates. The velocity across a ring panel appeared to be fairly uniform at different speeds and relatively unaffected by height (with the TSI probe positioned between 1 and 4 inches above the honeycomb). It appeared quite feasible to attempt a characterization of the entire air source ring using the TSI hot-wire probe. The characterization should utilize about 1000 measurements taken about 1 inch above the honeycomb, using an automated measurement process based on a LabView software program controlling a 2-m by 2-m x-y translator table.

CHARACTERIZATION OF THE AIR SOURCE

Introduction

The manual scoping measurements on the air inlet ring demonstrated a desirability to automate the characterization process. In order to automate the data collection for the air source, the TSI hot-wire anemometer was mounted onto a two-axis X-Y table. The table movement and data acquisition was controlled using PC based software. Thomson Industries made the x-y table and attached hardware. The rails are PN 2RB-M16-ODM and have 2 m of travel. The rails use a lead screw with a resolution of 0.0025 mm. The system uses OMNIDRIVE QDM-010i drives controlling BLX232 servomotors. The hardware control and data acquisition software was written using LabView 5.1.

Procedure and Results

All 16 panels were scanned using the pattern shown in Figure 15, starting in the lower left corner and finishing in the upper right corner, giving a total of 42 scan locations per panel. Data from each point within a small trapezoidal area was collected as follows. First a move to the point followed by a wait of 5 sec. Then 300 samples were taken (at 1500 samples/sec sample rate), from which a mean velocity and its standard deviation were calculated.

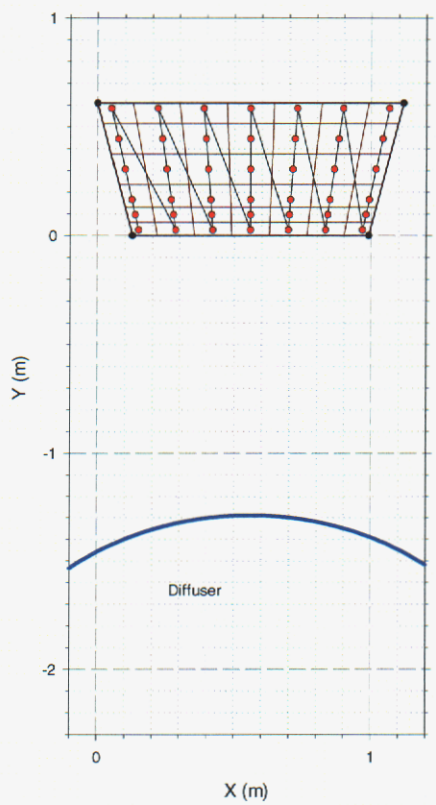

Figure 15. Locations for profiling one panel of the FLAME air source.

Table 4 shows the data collected for Panel 1with the blowers operated at 600 scfm. Table 4 gives for each scan location the position (in cartesian and cylindrical coordinates with 0,0 centered on the diffuser), the area of the trapazoid, and the velocity and the standard deviation. The X-Y table was reset to position 1 and the process was repeated at blower flow rates of 1000 scfm, 1500 scfm, 2000 scfm, and 4000 scfm. Ambient wind speed, direction, and temperature were also collected and archived. All 16 panels were characterized in this manner, as shown in Figure 16.

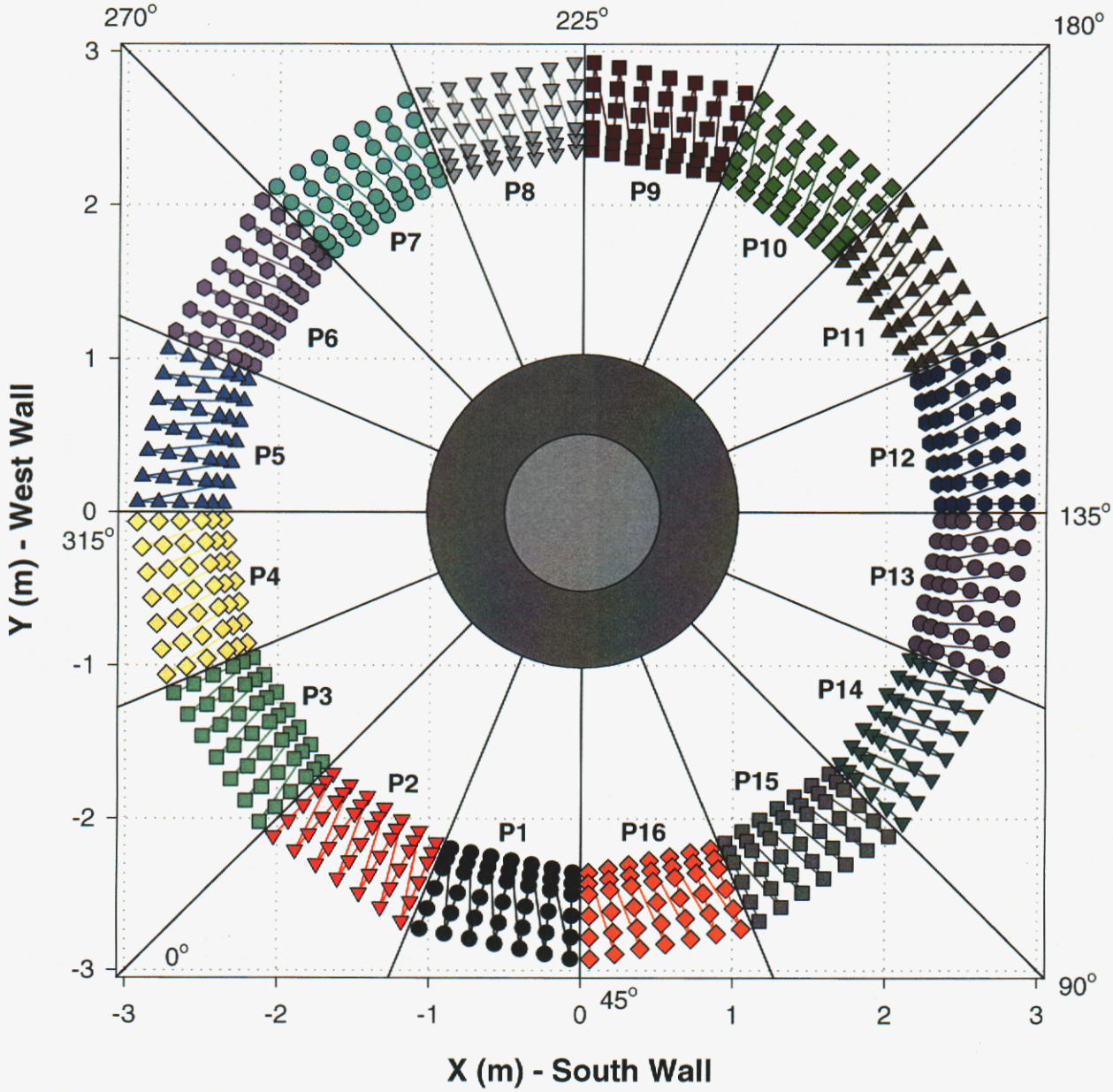

Figure 16. Hot-wire positions for air source characterization.

Table 4. Panel 1 Velocity Characterization Data at 600 SCFM Blower Flows

Position	X (m)	Y (m)	R (m)	Theta (deg)	Area (m^2)	Velocity (m/s)	Std.Dev. (m/s)
1	-0.052	-2.361	2.361	1.265	0.006	0.201	0.011
2	-0.054	-2.431	2.432	1.265	0.007	0.192	0.003
3	-0.055	-2.502	2.503	1.265	0.011	0.131	0.001
4	-0.058	-2.644	2.645	1.265	0.015	0.120	0.001
5	-0.062	-2.786	2.787	1.264	0.016	0.122	0.001
6	-0.065	-2.928	2.929	1.264	0.012	0.125	0.001
7	-0.185	-2.334	2.342	4.537	0.008	0.122	0.002
8	-0.191	-2.404	2.412	4.537	0.010	0.123	0.001
9	-0.196	-2.474	2.482	4.536	0.015	0.125	0.001
10	-0.207	-2.615	2.623	4.537	0.022	0.126	0.001
11	-0.219	-2.755	2.763	4.538	0.023	0.125	0.001
12	-0.230	-2.895	2.904	4.536	0.016	0.131	0.001
13	-0.319	-2.308	2.329	7.876	0.008	0.140	0.002
14	-0.329	-2.377	2.399	7.876	0.010	0.123	0.001
15	-0.338	-2.446	2.469	7.877	0.016	0.125	0.001
16	-0.358	-2.585	2.609	7.875	0.022	0.125	0.001
17	-0.377	-2.723	2.749	7.876	0.023	0.127	0.001
18	-0.396	-2.862	2.889	7.877	0.016	0.131	0.001
19	-0.454	-2.281	2.325	11.250	0.008	0.110	0.002
20	-0.467	-2.349	2.395	11.250	0.010	0.119	0.001
21	-0.481	-2.418	2.465	11.250	0.016	0.122	0.001
22	-0.508	-2.555	2.605	11.250	0.022	0.125	0.001
23	-0.535	-2.692	2.745	11.250	0.023	0.128	0.001
24	-0.563	-2.829	2.884	11.250	0.016	0.132	0.001
25	-0.588	-2.254	2.329	14.624	0.008	0.112	0.001
26	-0.606	-2.322	2.399	14.624	0.010	0.121	0.001
27	-0.623	-2.389	2.469	14.623	0.016	0.121	0.001
28	-0.659	-2.525	2.609	14.625	0.022	0.125	0.001
29	-0.694	-2.660	2.749	14.624	0.023	0.125	0.001
30	-0.729	-2.796	2.889	14.623	0.016	0.127	0.001
31	-0.722	-2.227	2.342	17.963	0.008	0.119	0.001
32	-0.744	-2.294	2.412	17.963	0.010	0.124	0.001
33	-0.766	-2.361	2.482	17.964	0.015	0.127	0.001
34	-0.809	-2.495	2.623	17.963	0.022	0.129	0.001
35	-0.852	-2.629	2.763	17.963	0.023	0.130	0.001
36	-0.896	-2.763	2.904	17.964	0.016	0.132	0.001
37	-0.855	-2.201	2.361	21.235	0.006	0.122	0.002
38	-0.881	-2.267	2.432	21.236	0.007	0.108	0.001
39	-0.907	-2.333	2.503	21.235	0.011	0.118	0.001
40	-0.958	-2.465	2.645	21.236	0.015	0.128	0.001
41	-1.009	-2.598	2.787	21.236	0.016	0.125	0.001
42	-1.061	-2.730	2.929	21.236	0.012	0.127	0.001

The mean panel velocity (weighed by area) was calculated using the trapezoidal area surrounding each measurement point (as shown in Figure 15).

$$V_{panel} = \sum_{i=1}^{42} \frac{V_i A_i}{A_{panel}} \qquad SD_{panel} = \sqrt{\frac{\sum_{i=1}^{42} (V_i - V_{panel})^2}{41}} \qquad Error_{panel} = \frac{SD_{panel}}{V_{panel}}$$

All panels had the same area, 0.6039 m^2. Table 5 gives the average velocity, standard deviation, and standard error for each panel with the blowers set at 600 scfm. The calculations for the entire air source ring (All Panels below) were similar (assuming 42x16 individual points, not separated by panels).

Table 5. Velocity Characterization Data for All Panels at 600 SCFM Blower Flows

Panel	Vave (m/s)	Std. Dev. (m/s)	Std. Error
1	0.127	0.017	0.131
2	0.131	0.007	0.056
3	0.135	0.017	0.128
4	0.123	0.010	0.082
5	0.121	0.010	0.086
6	0.119	0.016	0.132
7	0.126	0.015	0.115
8	0.118	0.019	0.161
9	0.118	0.008	0.068
10	0.117	0.016	0.133
11	0.124	0.029	0.232
12	0.119	0.006	0.050
13	0.112	0.011	0.102
14	0.125	0.013	0.102
15	0.117	0.009	0.080
16	0.135	0.035	0.259
All panels	**0.123**	**0.018**	**0.145**

Appendix B provides similar tables (B1-B10) for all 16 panels at blower flow rates of 1000, 1500, 2000, and 4000 SCFM. Blower flow rate information, and wind speed and direction are also included in Appendix B. The blower controllers functioned extremely well with little deviation from the desired flow rates.

Figures 17 through 21 present 3-D and planar velocity contours of all panels at the 5 blower flow rates. Contour levels are centered on the average velocity with a contour range set at 3 standard deviations (from Table 8). Figure 22 compares the 3-D velocity profiles at the 5 blower flow rates.

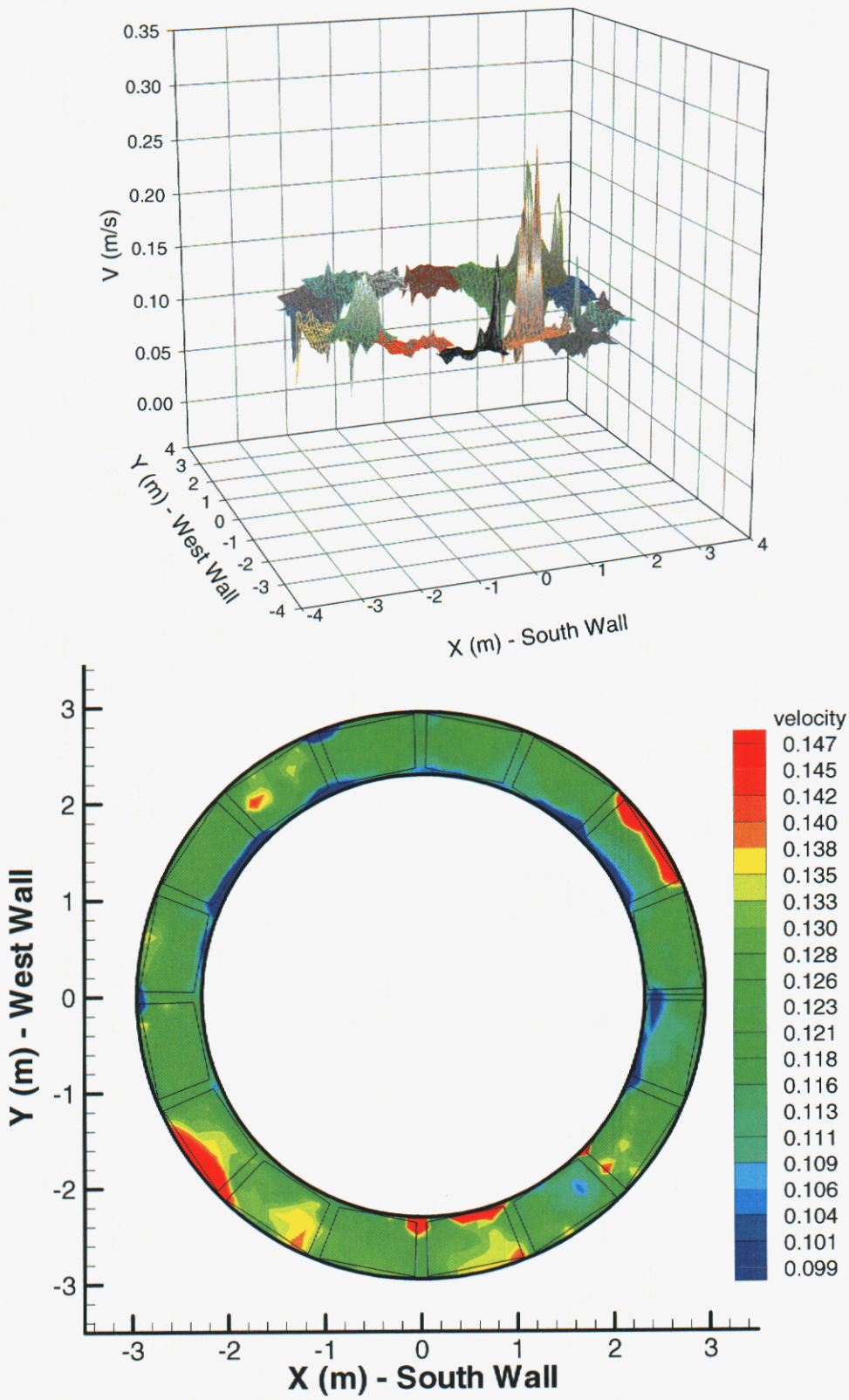

Figure 17. Air source velocity contours with blowers at 600 scfm.

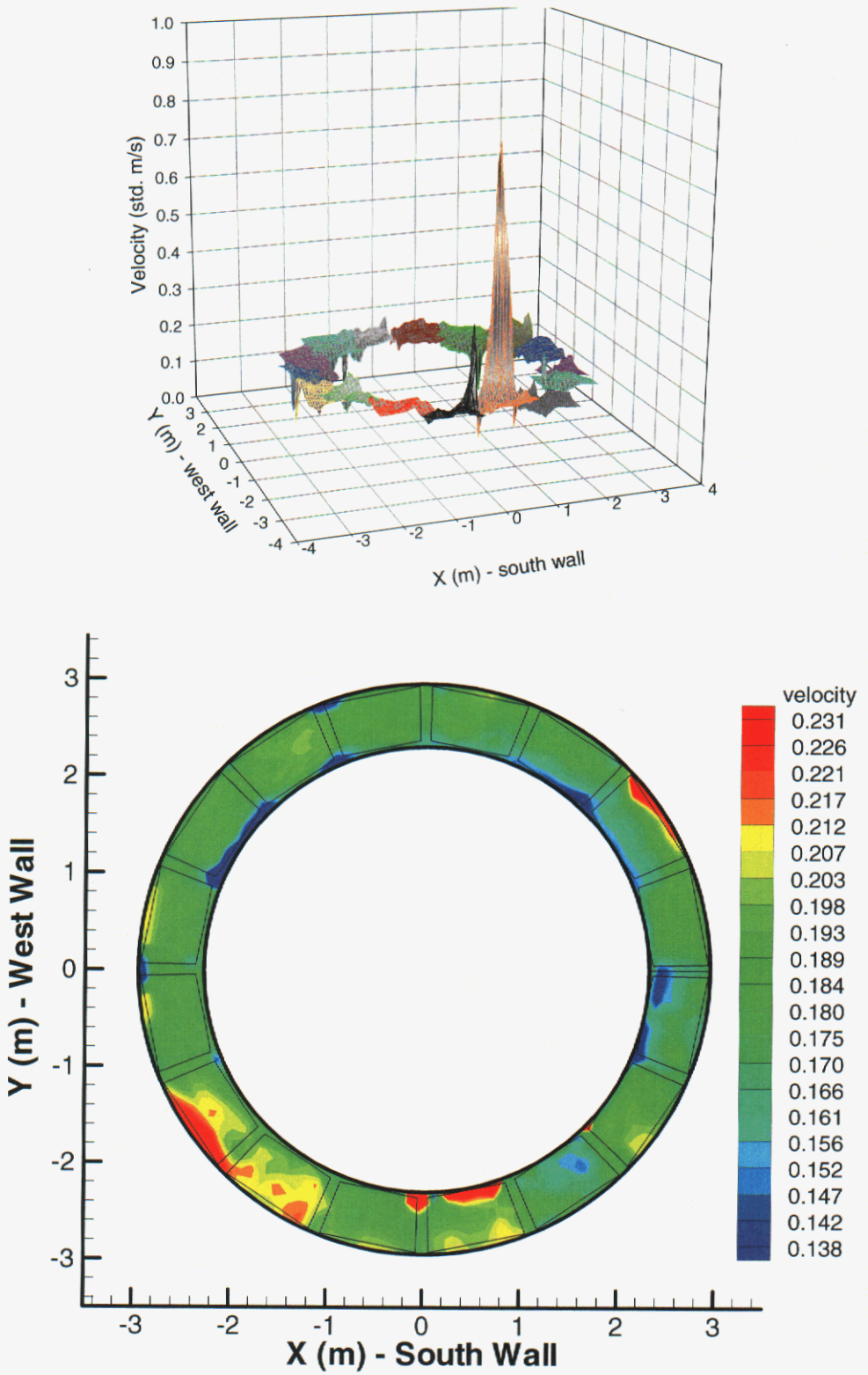

Figure 18. Air source velocity contours with blowers at 1000 scfm.

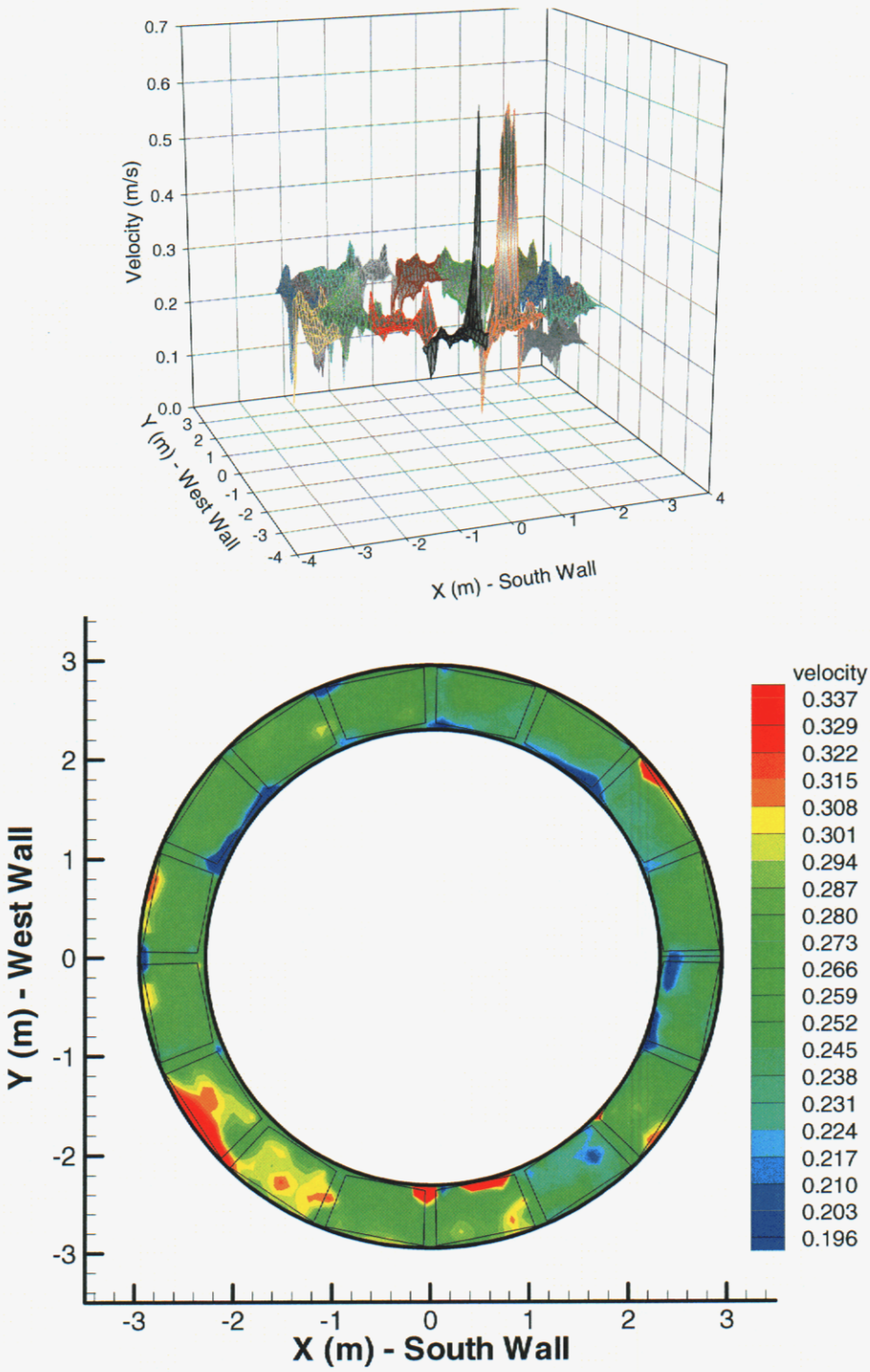

Figure 19. Air source velocity contours with blowers at 1500 scfm.

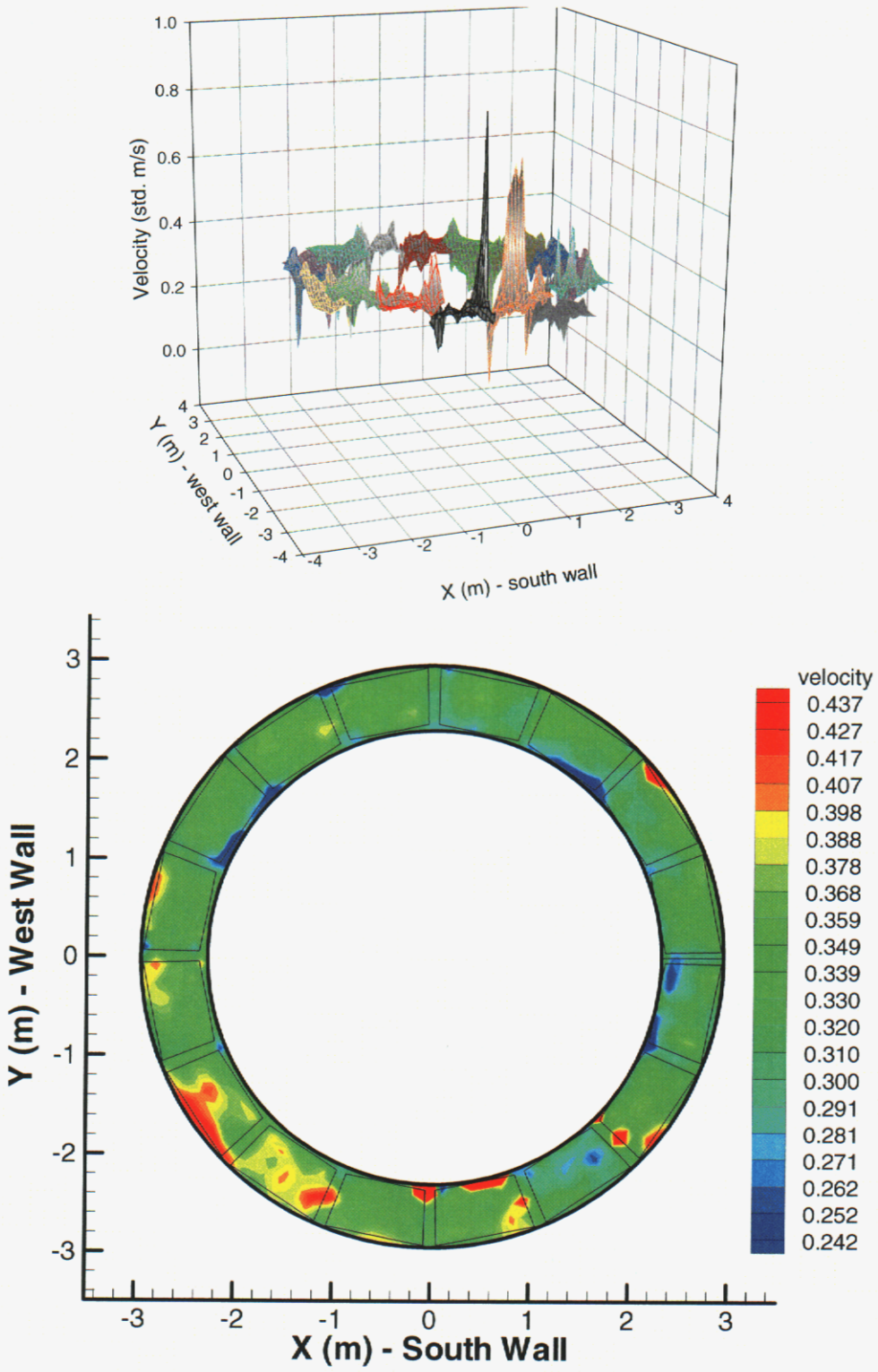

Figure 20. Air source velocity contours with blowers at 2000 scfm.

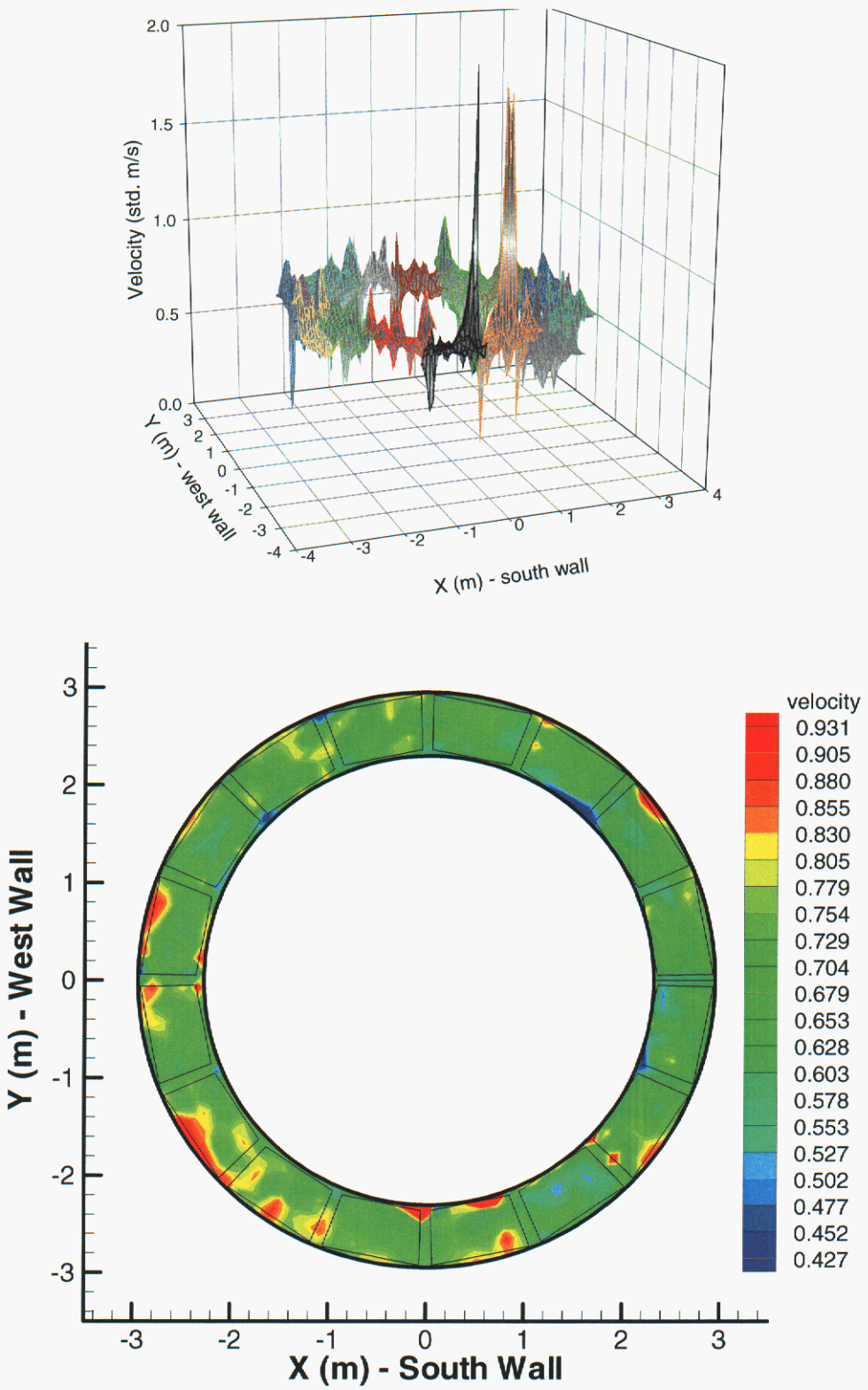

Figure 21. Air source velocity contours with blowers at 4000 scfm.

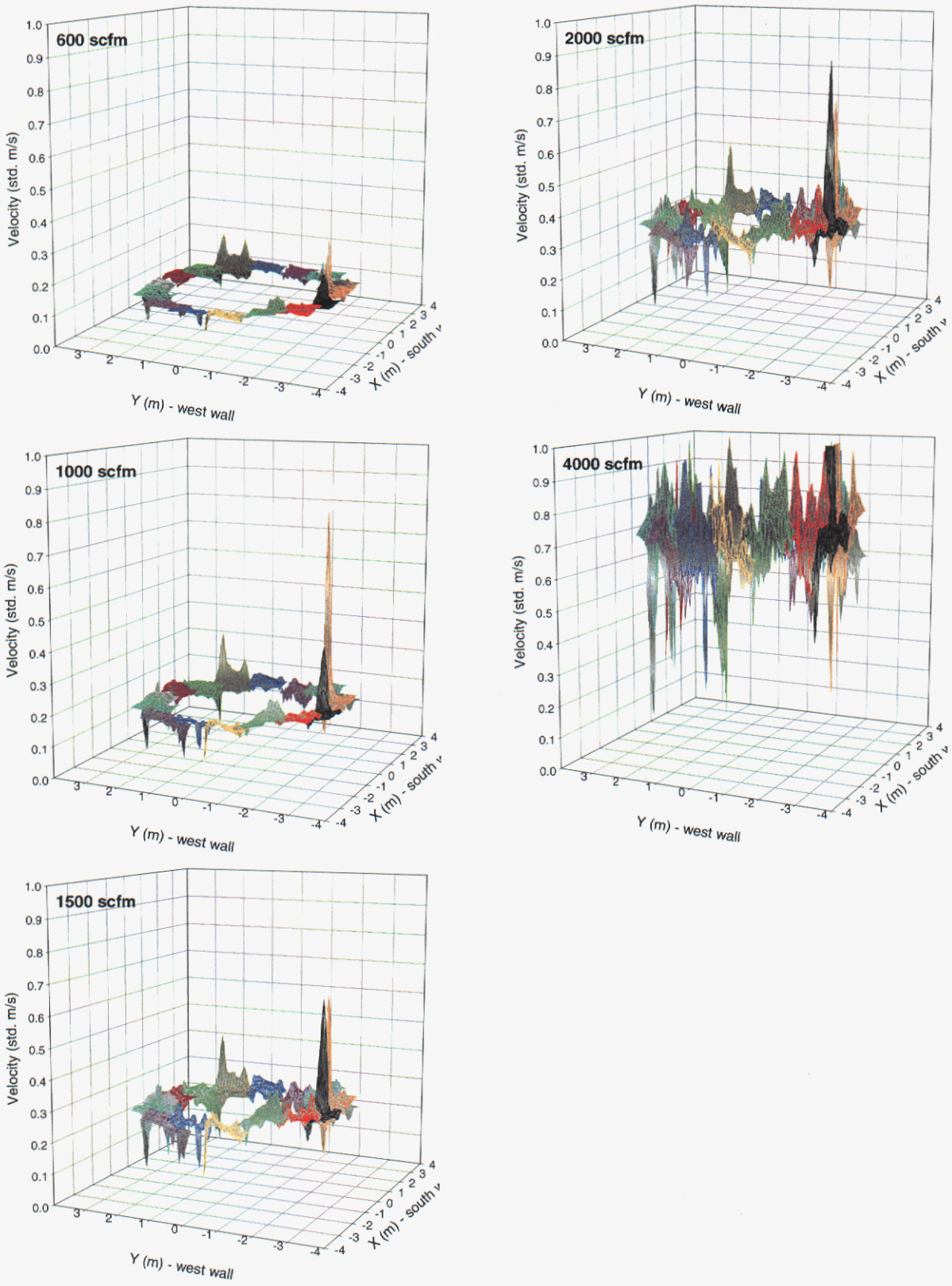

Figure 22. Air source panel velocity profiles at 5 blower speeds.

Figure 23 plots the standard error of the velocity for each panel at the various blower flow rates. The standard error for the panels ranges from 15% to 25%.

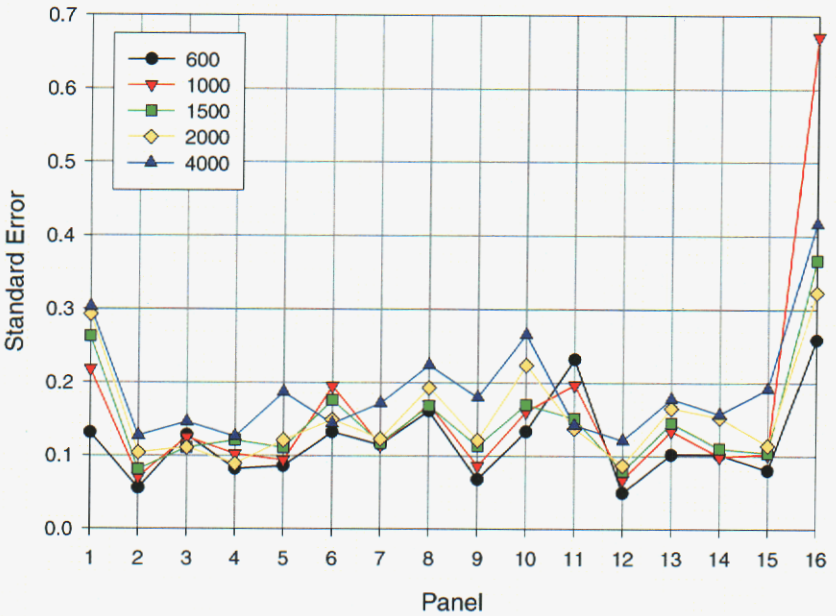

Figure 23. The standard error of the velocity for each panel at the various blower flow rates.

Table 6 gives the average velocity (in standard m/s) at various blower flow rates for the total air source from the combined panels and the four ganged blowers, along with the standard deviation and error.

Table 6. Average Air Source Velocity as a function of the ganged blower speed.

Blower Speed (scfm)	Average Velocity (smps)	Standard Deviation (m/s)	Standard Error
600	0.1229	0.0179	0.1453
1000	0.1843	0.0469	0.2543
1500	0.2644	0.0493	0.1865
2000	0.3382	0.0633	0.1872
4000	0.6922	0.1517	0.2191

"Hot" and "cold" spots in the flow, shown in Figures 18-21 (predominately in panels 1 and 16), tended to skew the ring average error somewhat. Due to fabrication tolerances, small-scale features (on the order of square centimeters) around joints and edges of the 3 mm cell diameter, 5 cm deep honeycomb panels at the exit of the air ducts caused the variation. Analysis of the spatial distribution without these hot spots showed that segment-to-segment variation over the 16 segments that make up the air duct is +/- 10%. Figures 24 and 25 and Tables 7 and 8 show the results when discarding the sensor data for each panel ID, OD, and side edges (see Figure 15 for sensor locations).

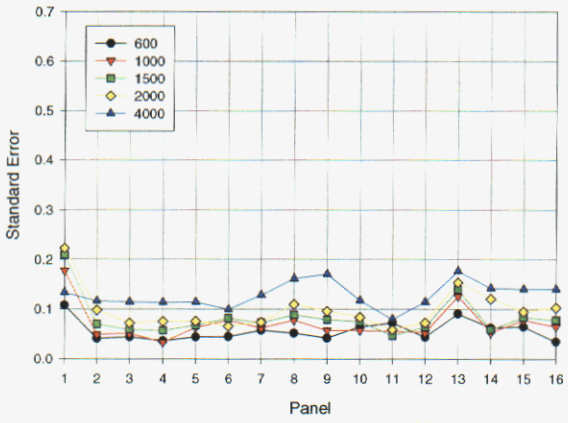

Figure 24. The standard error of the velocity for each panel (without panel ID and OD edges).

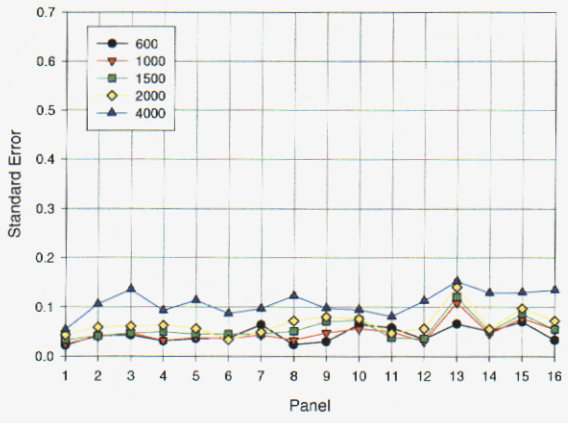

Figure 25. The standard error of the velocity for each panel (without panel ID and OD and side edges).

Table 7. Average Air Source Velocity as a function of the ganged blower speed. (without panel ID and OD edges)

Blower Speed (scfm)	Average Velocity (smps)	Standard Deviation (m/s)	Standard Error
600	0.123	0.009	0.074
1000	0.183	0.019	0.103
1500	0.263	0.030	0.114
2000	0.337	0.043	0.126
4000	0.679	0.098	0.145

Table 8. Average Air Source Velocity as a function of the ganged blower speed. (without panel ID and OD and side edges)

Blower Speed (scfm)	Average Velocity (smps)	Standard Deviation (m/s)	Standard Error
600	0.123	0.008	0.065
1000	0.184	0.016	0.084
1500	0.266	0.024	0.088
2000	0.339	0.032	0.095
4000	0.679	0.084	0.124

An excellent fit (r^2=0.998) of the velocity data can be made using a 1st order regression, with the fit parameters and 95% confidence interval shown in Figure 26.

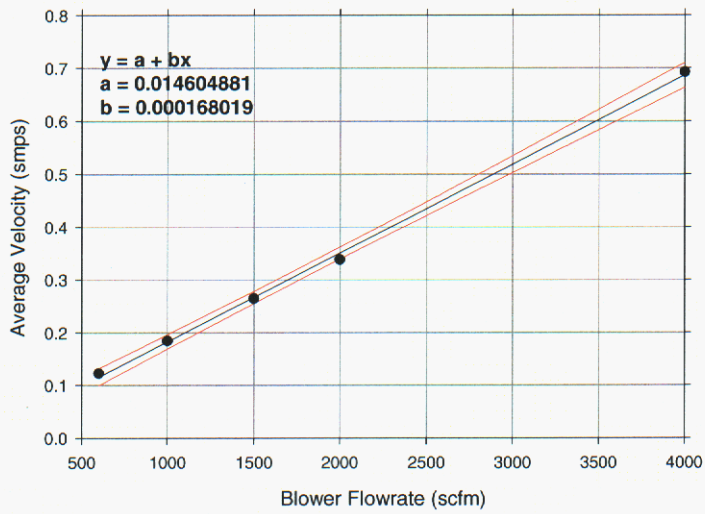

Figure 26. FLAME air source velocity as a function of the ganged blower flow rates.

Conclusions

The air source (sixteen separate panels fed by four blowers and attached ductwork) was fully characterized using an automated data collection process. Velocity data was taken at 672 circumferential locations across the entire air source ring and at five different blower flow rates. A standard deviation and the standard error were computed for each measurement point. This point data was used to compute average velocity for each panel and therefore the entire ring. A first order regression showed that the air source velocity in FLAME was a linear function of the ganged blower flow rates:

$$V(smps) = 0.000168 \times BlowerFlowrate(scfm) + 0.014605$$

This page intentionally left blank.

CHARACTERIZATION OF THE PLUME SOURCE

Introduction

Characterization of the plume source was performed mainly to determine the uniformity of the plume exit flow for previous and upcoming PIV/PLIF experiments. The plume source characterization was performed in a similar manner as with the air source characterization, with the only exceptions being four TSI probes were mounted to the X-Y table and the scan was performed in only one direction.

Gas manifold pressure regulators and associated flow controllers control the plume source exit velocity. With only twelve 44 L high-pressure gas cylinders capable of being mounted to the gas manifold, time was of the essence in data collection. It was desired to take data for three average velocities, 0.1, 0.2, and 0.3 m/s; it would be necessary to take the data within 12 min., 6 min., and 3 min., respectively, before the gas would be depleted.

Procedure and Results

Figure 27 shows the test setup for characterization of the plume source. Twelve air cylinders were attached to the high-pressure gas manifold. The flow was measured using calibrated FlowMetrics FM-16M50 turbine meters, Endevco 8530B strain gage pressure transducers, and K-type thermocouples. For the 0.1 m/s plume source characterization, flow was controlled by the fuel line regulator and its Jordan valve (approximately 73% open).

Figure 27. Scanning the plume source with 4 TSI hot-wire probes on 6-ft X-Y table.

Figure 28 shows that for the 0.1 m/s scan measurement points were 5 cm apart in the y direction (+55 cm to –55 cm). The spacing in x was 12.5 cm. The probes were located between 5-10 cm above the source exit. Two separate scans (left and right sides of the diffuser) were performed, yielding a total of 184 measurement locations.

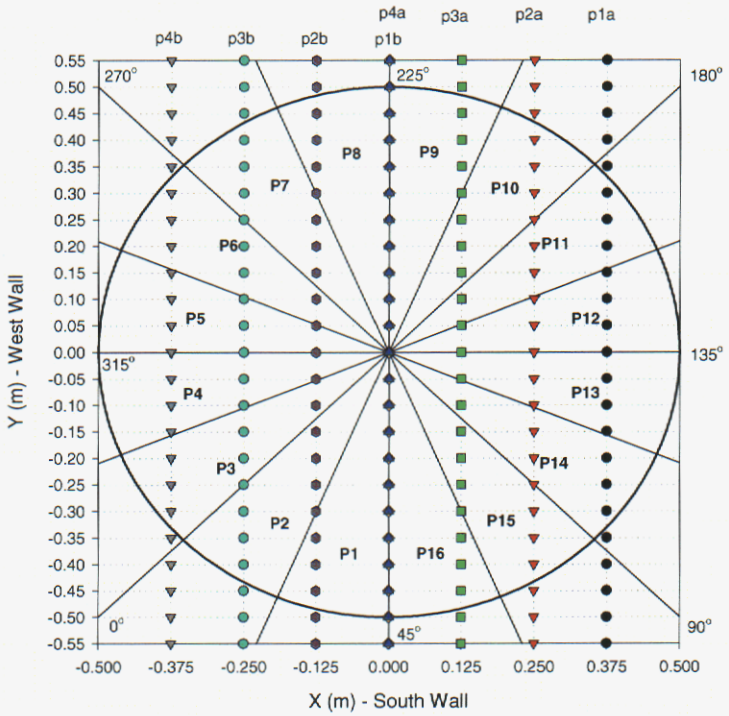

Figure 28. TSI probe positions for 0.1 m/s velocity characterization of plume source.

The data reduction is of interest. Figures 29 through 31 show the measured gas volumetric flow, pressure, and temperature in the fuel line for the 0.1 m/s plume (similar data was taken for the 0.2 and the 0.3 m/s plume flows). The volumetric flowmeters and the gas manifold pressure transducers were calibrated just prior to the testing.

Gas temperature at the diffuser exit is also shown in Figure 31. Figures 32 and 33 present the calculated gas densities in the gas line and at the diffuser exit and also the calculated gas mass flow rate. These values are then used to estimate the actual and the standard gas velocity at the diffuser exit (standard velocity is calculated to allow direct comparison with the TSI probe measured values).

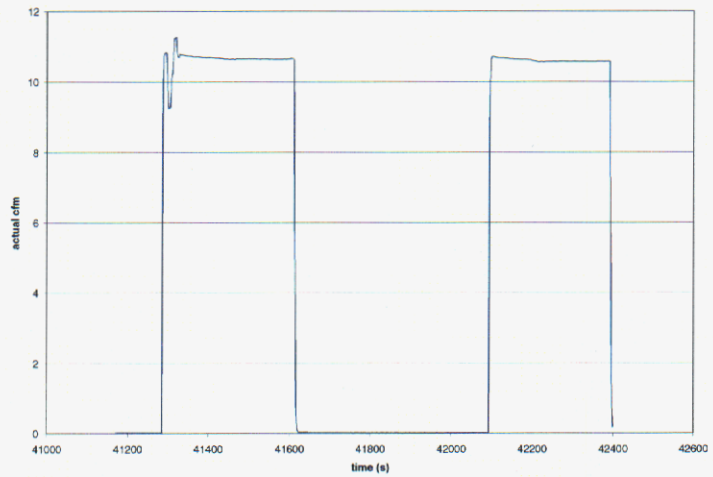

Figure 29. Gas line volumetric flow rate in the 0.1 m/s plume source characterization.

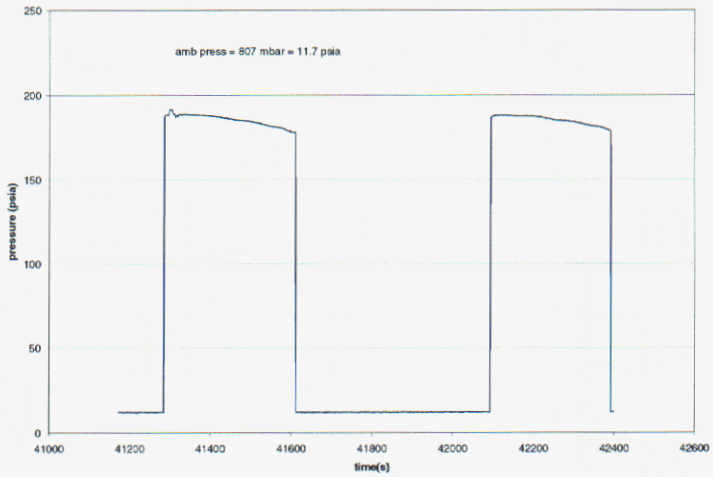

Figure 30. Gas line pressure in the 0.1 m/s plume source characterization.

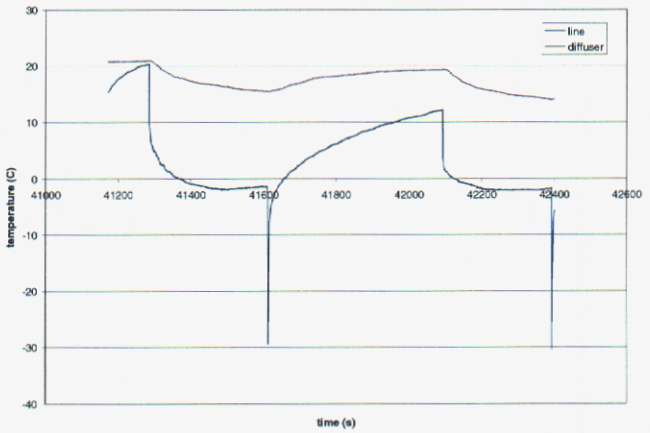

Figure 31. Gas line and diffuser exit temperatures in the 0.1 m/s plume source characterization.

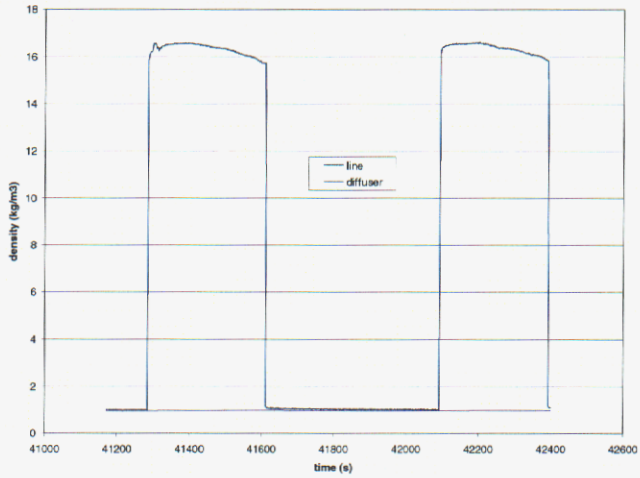

Figure 32. Gas line and diffuser exit densities in the 0.1 m/s plume source characterization.

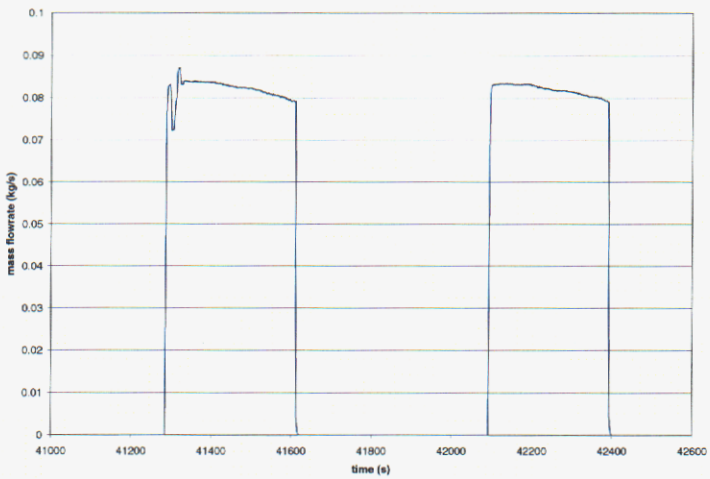

Figure 33. Mass flow rate (line and diffuser) in the 0.1 m/s plume source characterization.

The equations below give the data reduction methodology:

$$\rho_{line} = \frac{P_{line}}{RT_{line}}$$

$$\rho_{diffuser} = \frac{P_{ambient}}{RT_{diffuser}}$$

$$\dot{m}_{line} = Q_{line} \times \rho_{line} = \dot{m}_{diffuser}$$

$$V_{actual} = \frac{\dot{m}_{diffuser}}{\rho_{diffuser} A_{diffuser}}$$

$$V_{s\tan dard} = V_{actual} \times \frac{P_{ambient}}{P_{s\tan dard}} \times \frac{T_{s\tan dard}}{T_{diffuser}}$$

where:

ρ_{line}	=	line gas density, (kg/m^3)
$\rho_{diffuser}$	=	diffuser exit gas density, (kg/m^3)
T_{line}	=	line gas temperature, (K)
$T_{diffuser}$	=	diffuser exit gas temperature, (K)
$T_{standard}$	=	TSI probe standard temperature, 21.1 °C, (294 K)
P_{line}	=	line pressure, (psia)
$P_{diffuser}$	=	diffuser exit pressure (psia), assumed equal to $P_{ambient}$
$P_{ambient}$	=	807 mbar, (11.7 psia)
$P_{standard}$	=	TSI probe standard pressure, 1013 mbar, (14.7 psia)
Q_{line}	=	line volume flow rate, (actual m^3/s)
$A_{diffuser}$	=	0.785 m^2 (1-m diameter) * 0.92
$\dot{m}_{line}$	=	line mass flow rate (kg/s), assumed equal to $\dot{m}_{diffuser}$
V_{actual}	=	diffuser exit gas velocity, (actual m/s)
$V_{standard}$	=	diffuser exit gas velocity, (standard m/s)
R_u	=	universal gas constant, (0.008314 bar m^3 / kg·mol K)
M	=	air gas molar mass, (28.97 kg/ kg·mol)
R	=	Gas constant $= \frac{R_u}{M}$, (0.0416 psia m^3 / kg K).

The diffuser area was reduced by correction factor of 0.08 to account for the honeycomb (304 stainless steel foil ribbon construction). Figure 34 compares the TSI probe measured velocity (standard m/s) to the calculated velocity (standard m/s) based on gas line parameters. For this condition, the TSI probe is slightly below its operating range and the associated uncertainty may be larger than ± 2%. It is immediately evident that the flow field changed with time (and hence location). This was caused by the pressure regulator, which could not quite maintain the set pressure (200 psia) as the source gas depleted and the upstream manifold pressure decreased.

Ignoring this effect would introduce error when calculating the uniformity of the flow field. The velocity measurement taken at the diffuser South end (later in time than the North end measurements) would be skewed lower. To correct this, the slope of the calculated standard velocity (during the TSI probe measurement time) was determined. This slope was then subtracted from the calculated standard velocity as well as the measured data. This correction is not shown in Figure 34. After correcting for the pressure drop, the calculated average air velocity, standard deviation, and standard error were 0.097 m/s (standard), 0.0005 m/s, and 0.005, respectively, using the 508 gas line measurements that were taken only when the probe was within the diffuser plane.

Figure 35 presents velocity contours of the TSI probe data after adjusting for pressure decay in the gas line. The measured average air velocity, standard deviation, and standard error were 0.119 m/s (standard), 0.004 m/s, and 0.032, respectively, using 117 measurements located inside

the diffuser plane. The measured velocity was about 23% greater than calculated using gas line data.

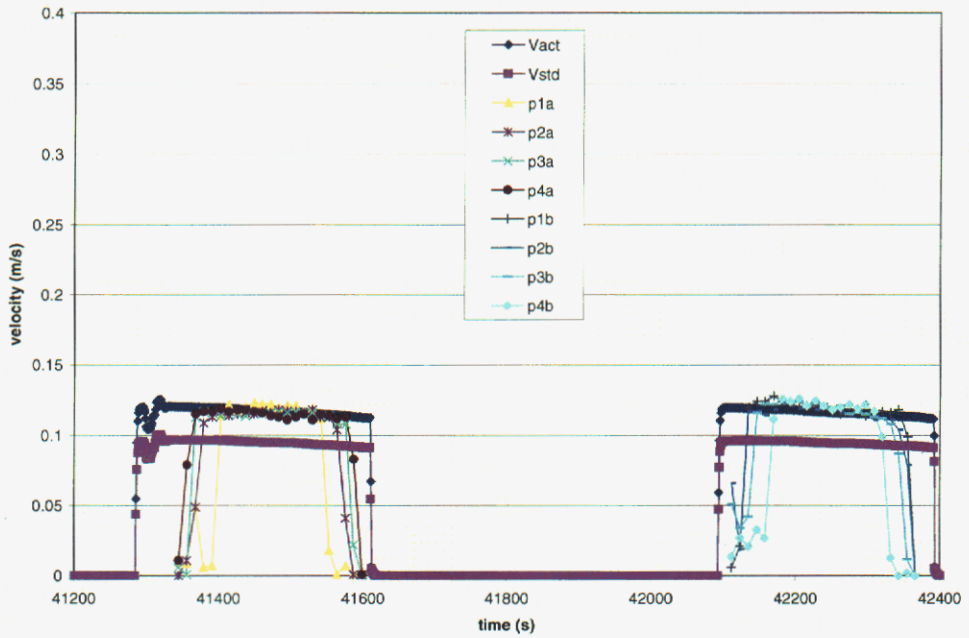

Figure 34. Calculated Vact and Vstd compared to TSI Vstd data for 0.1 m/s plume source.

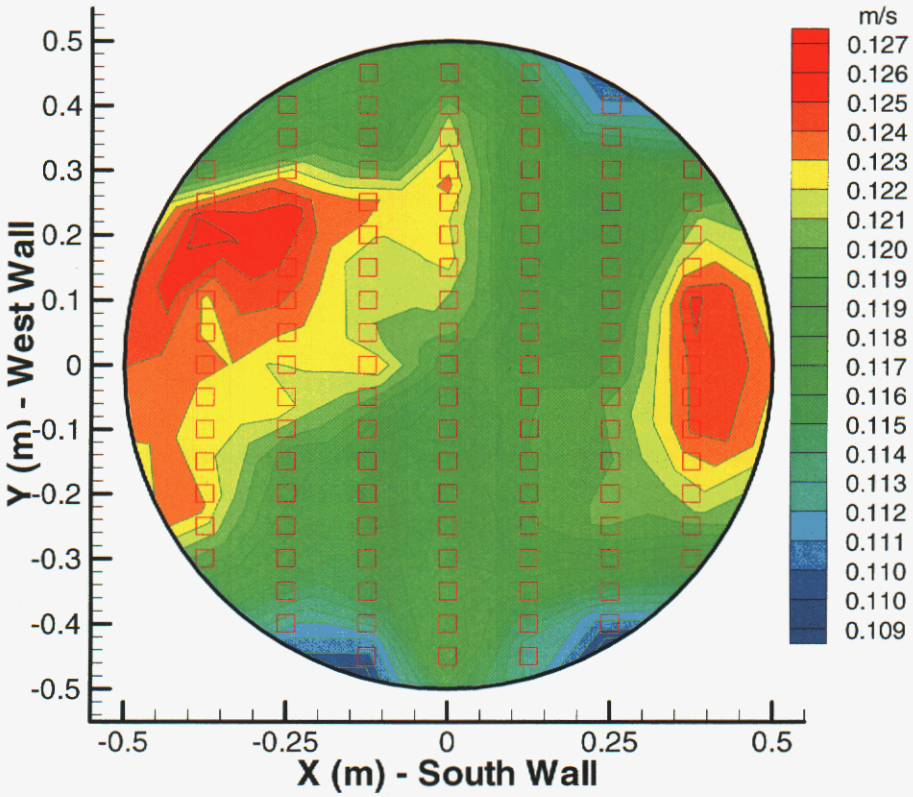

Figure 35. The 0.1 m/s plume source adjusted for line pressure decay.

Figure 36 shows that the 0.2 m/s characterization was performed using only one North to South scan; the spacing in x was increased. Measurement points were 5 cm apart in the y direction (+55 cm to –55 cm). The spacing in x was 20 cm. The Jordan valve was opened about 93%. Figure 37 compares the TSI measured velocity compared to the calculated velocity (uncorrected for pressure decay).

The calculated average air velocity, standard deviation, and standard error were 0.177 m/s (standard), 0.0003 m/s, and 0.001, respectively, using the 148 gas line measurements that were taken only when the probe was within the diffuser plane.

Figure 38 presents velocity contours of the TSI probe data after adjusting for pressure decay in the gas line. The measured average air velocity, standard deviation, and standard error were 0.189 m/s (standard), 0.008 m/s, and 0.044, respectively, using 68 measurements located inside the diffuser plane. The measured velocity was about 7% greater than calculated using gas line data.

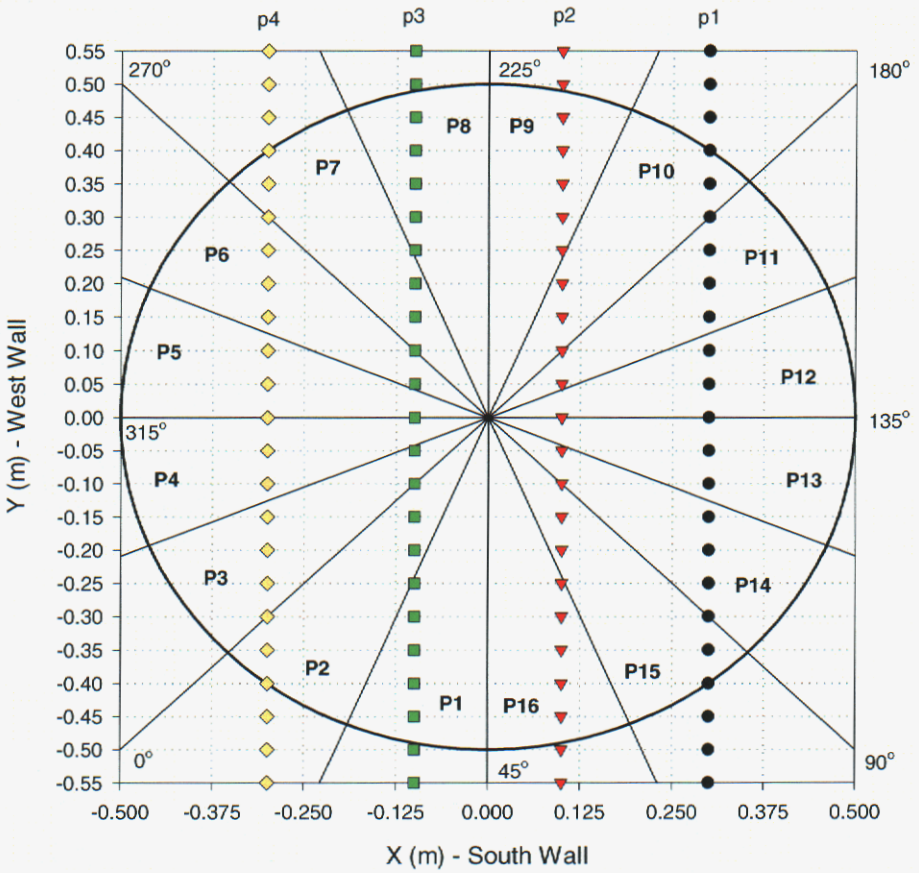

Figure 36. TSI probe positions for 0.2 m/s velocity characterization of plume source.

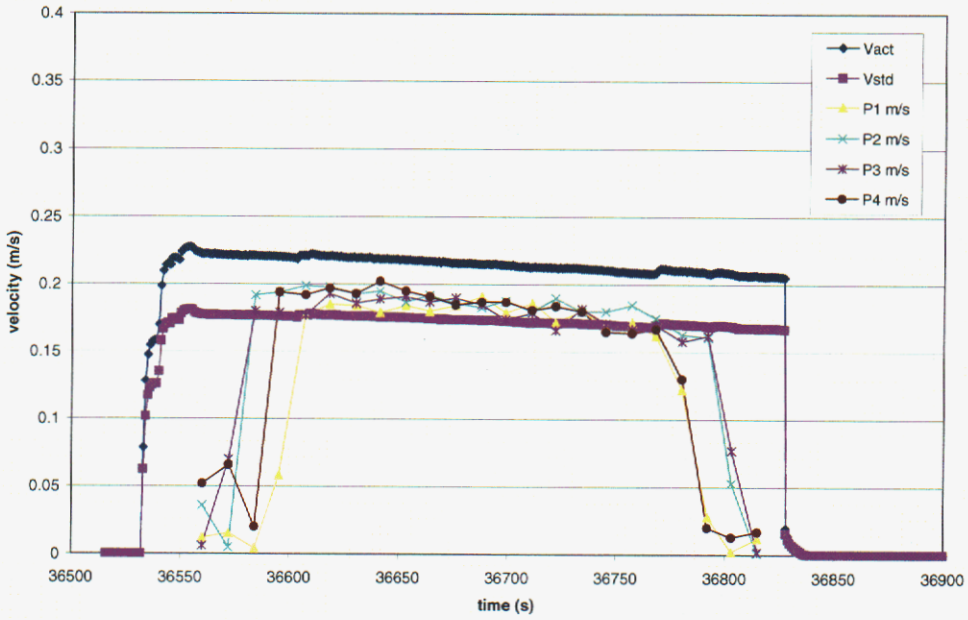

Figure 37. Calculated Vact and Vstd compared to TSI Vstd data for 0.2 m/s plume source.

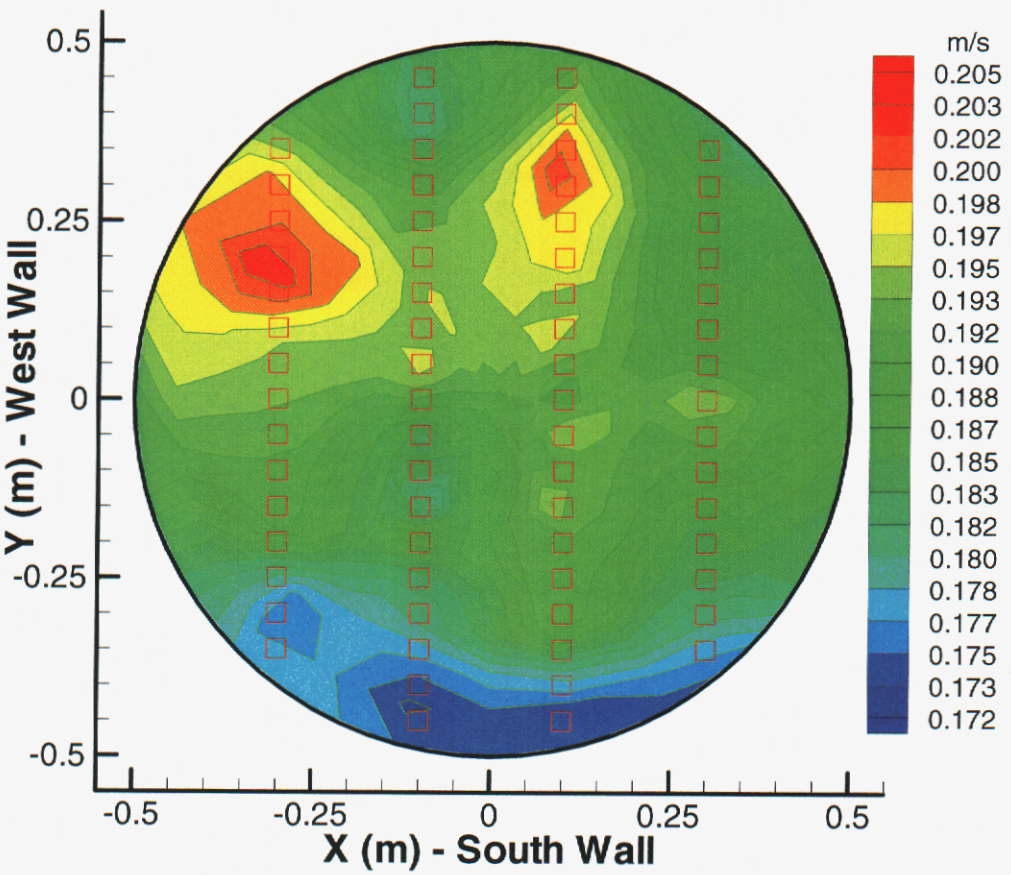

Figure 38. The 0.2 m/s plume source adjusted for line pressure decay.

Figure 39 shows that the 0.3 m/s characterization was also performed using only one North to South scan. Measurement points were 10 cm apart in the y direction (+60 cm to –50 cm). The spacing in x was 20 cm. The Jordan valve for the fuel line manifold was opened about 98%. Because additional gas flow time was needed, the diluent line was also made operational. The Jordan valve for the diluent line manifold was opened about 60%. Figure 40 compares the TSI measured velocity compared to the calculated velocity (uncorrected for pressure decay).

The calculated average air velocity, standard deviation, and standard error were 0.254 m/s (standard), 0.0006 m/s, and 0.002, respectively, using the 143 gas line measurements that were taken only when the probe was within the diffuser plane.

Figure 41 present velocity contours made using the TSI probe data after adjusting for pressure decay in the gas line. The measured average air velocity, standard deviation, and standard error were 0.288 m/s (standard), 0.012 m/s, and 0.042, respectively, using 32 measurements located inside the diffuser plane. The measured velocity was about 13% greater than calculated using gas line data.

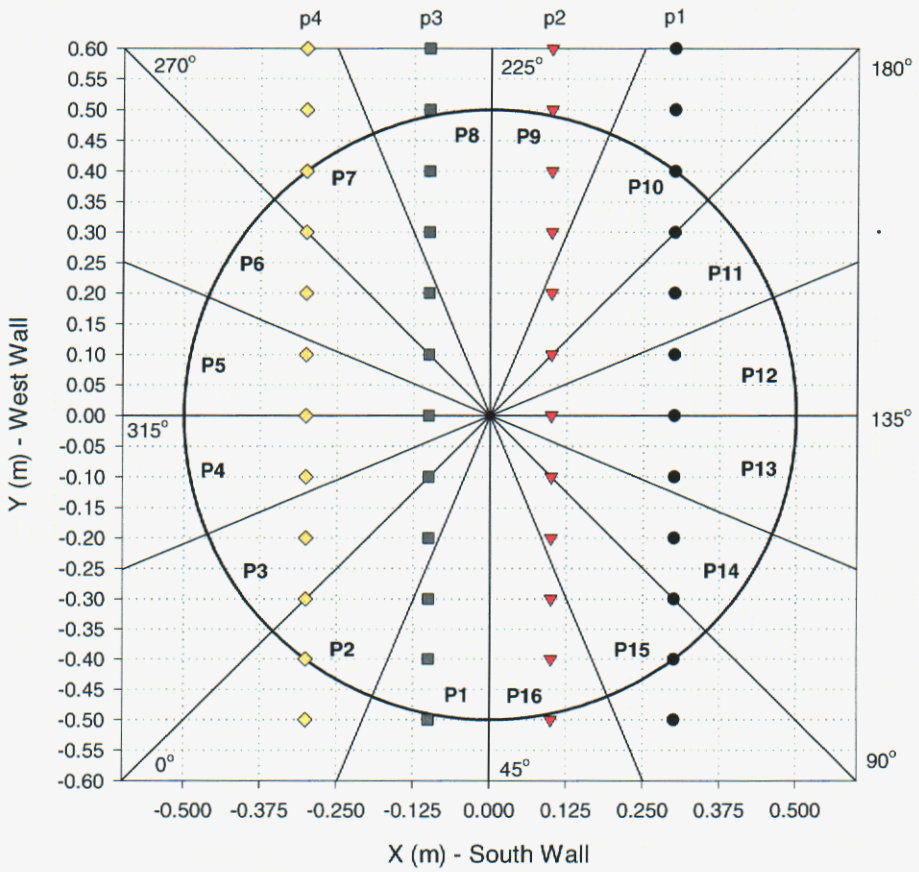

Figure 39. TSI probe positions for 0.3 m/s velocity characterization of plume source.

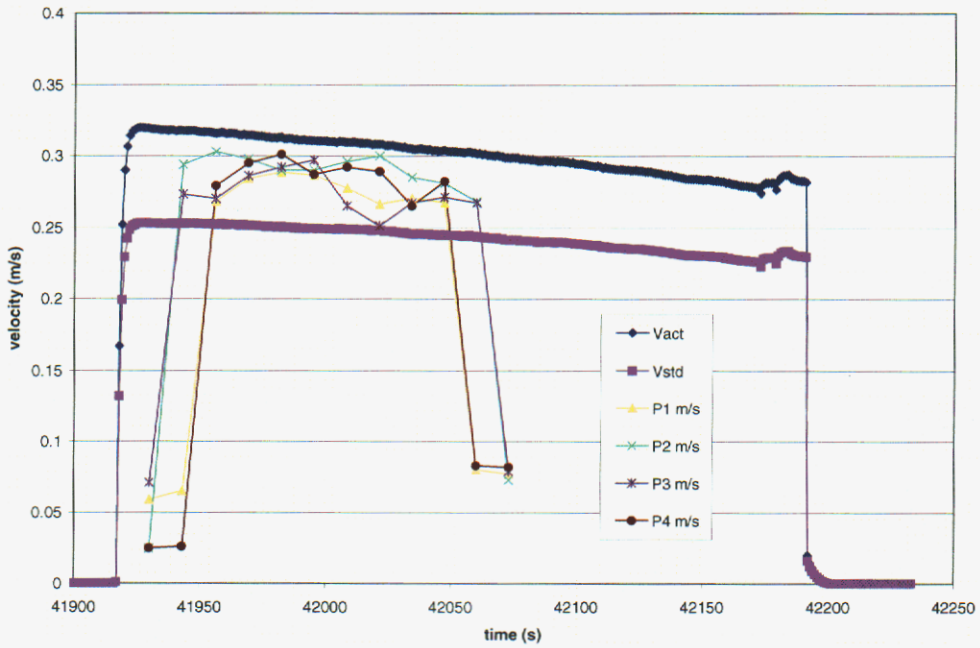

Figure 40. Calculated Vact and Vstd compared to TSI Vstd data for 0.3 m/s plume source.

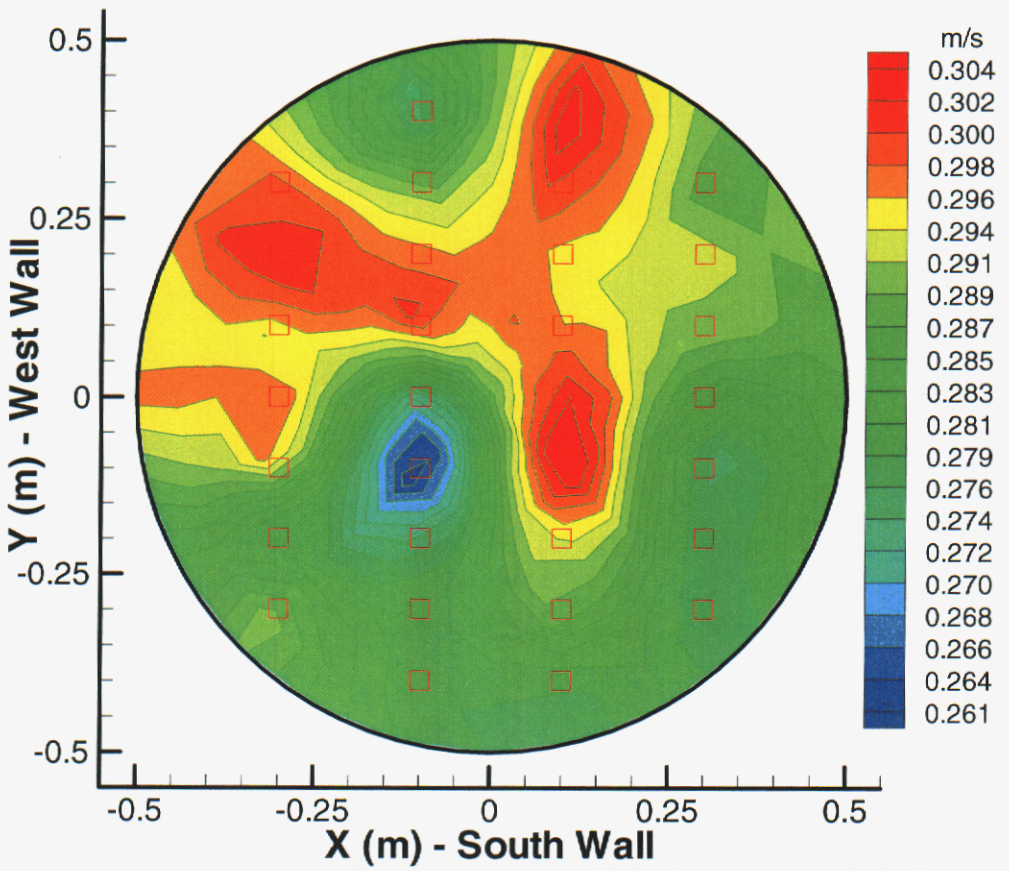

Figure 41. The 0.3 m/s plume source adjusted for line pressure decay.

Conclusions

The plume source was characterized at three nominal velocities, 0.1, 0.2, and 0.3 m/s. Table 9 presents the comparisons.

Table 9. Plume Source Results

Nominal Velocity (standard m/s)	0.1	0.2	0.3
Calculated Velocity (standard m/s)	0.097	0.177	0.254
Measured Velocity (standard m/s)	0.119	0.189	0.288
Standard Deviation (m/s)	0.004	0.008	0.012
Standard Error	0.032	0.044	0.042

The first, and most important observation, is that the plume source is quite uniform. The standard error shows only about 3-4% variation in velocity across the entire diffuser exit plane, at the three velocities characterized.

The second observation is that the measured velocity is always greater than that calculated based on line measurements, varying between 23% and 7% (with the largest difference at the lowest velocity). Studies of discharge coefficients through perforated plates at low Reynolds numbers (Smith et al. 1958) indicate that the discharge coefficient for the aluminum honeycomb may be on the order of 0.8-0.9 (increasing with the Re number). Applying these coefficients would increase the calculated velocity by 25-11%. It must be noted that the above estimates for the honeycomb discharge coefficients are outside the correlation (correlation parameters: minimum Re number = 400, plate thickness-to-hole diameter = 2, pitch-to-hole diameter = 2; honeycomb parameters: minimum Re number = 25, plate thickness-to-hole diameter = 27, pitch-to-hole diameter ~ 1).

This page intentionally left blank

SUMMARY

The Fire Laboratory for the Accreditation of Models and Experiments (FLAME) is being used to acquire data sets for buoyant, non-reacting, and reacting flows of sufficient quality to support validation of numerical simulation tools. To achieve this goal, not only must simultaneous temporal and spatial imaging with sufficient resolution be obtained for the flow of interest, but the geometry, initial conditions, and boundary conditions must also be specifiable with sufficient resolution.

First, it was determined that the standard error in velocity in the four inlet ducts feeding the air source was quite small (about 5%) for each speed and each blower. A curve was determined that yielded the volumetric flow rate as a function of the voltage measured by the permanently installed Kurz anemometer for each blower and associated duct. These curves were installed in the LabView© blower operation program at FLAME, enabling accurate and stable flow rates from each blower.

Second, with the blowers ganged to yield identical flow rates, the velocity across a ring panel was found to be fairly uniform at different speeds and relatively unaffected by height (between 1 and 4 inches above the honeycomb). The air source (sixteen separate panels fed by four blowers and attached ductwork) was fully characterized using an automated data collection process (672 measurements taken about 1 inch above the honeycomb, using an automated measurement process based on a LabView software program controlling a 2-m by 2-m x-y translator table). Velocity data was taken at five different blower flows rates. A standard deviation and the standard error were computed for each measurement point. This point data was used to compute average velocity for each panel and therefore the entire ring. A first order regression showed that the air source velocity in FLAME was a linear function of the ganged blower flow rates. The standard error for the average velocity of the air source ranged between 12-25% over the five blower flows. Fabrication tolerances caused small "hot spots" (small-scale features on the order of square centimeters around joints and edges of the 3-mm cell diameter, 5-cm deep honeycomb panels at the exit of the air ducts). Discarding the "hot spot" data yielded a spatial velocity distribution within +/- 10% of the air source ring average.

The plume source was characterized using the automated characterization technique. A detailed posttest analysis of the spatial velocity distribution (average measurement spacing – 0.09 m) of the burner (using an airflow) shows that the velocity profile is flat. The standard error shows only about 3-4% variation in velocity across the entire diffuser exit plane, at the three velocities characterized.

Analysts can now be provided with a reasonable set of boundary condition measurements for the current and future series of experiments utilizing particle image velocimetry (PIV) for velocity field measurements and planar laser induced fluorescence (PLIF) for scalar field measurements. Also, operators and experimenters of FLAME have been given a knowledge-based database to allow controlling the boundary conditions with some repeatability.

This page intentionally left blank

REFERENCES

1. Tieszen, Sheldon R., Timothy J. O'Hern, Robert W. Schefer, and Leroy D. Perea, *Spatial and Temporal Resolution of Fluid Flows: LDRD Final Report,* SAND98-0338, Sandia National Laboratories, February 1998.

2. Smith, P. L., Jr., and Matthew Van Winkle, *Discharge Coefficients Through Perforated Plates at Reynolds Numbers of 400 to 3000,* AiChE Journal, Vol. 4, No. 3, 1958.

This page intentionally left blank

APPENDIX A
Blower and Duct Characterization Data

Table A1. NW Blower Duct Spatial Velocity at Five Blower Speeds

X (inch)	Y (inch)	Velocity (smps) 1 volt	Velocity (smps) 2 volt	Velocity (smps) 3 volt	Velocity (smps) 4 volt	Velocity (smps) 5 volt
3.0	21.0	0.90	1.87	2.68	3.70	5.10
3.0	15.0	1.02	1.93	2.93	4.09	5.36
3.0	9.0	0.97	1.92	2.91	3.89	4.99
3.0	3.0	0.91	1.83	2.74	3.64	4.72
9.0	21.0	0.81	1.66	2.60	3.40	4.57
9.0	15.0	0.98	1.80	3.11	4.25	5.53
9.0	9.0	0.98	2.02	3.03	3.95	5.19
9.0	3.0	0.88	1.82	2.81	3.72	4.83
15.0	21.0	0.71	1.67	2.63	3.54	4.53
15.0	15.0	1.00	2.03	3.09	4.22	5.50
15.0	9.0	1.00	1.96	2.98	4.12	5.25
15.0	3.0	0.92	1.95	2.94	3.95	5.01
21.0	21.0	0.70	1.78	2.68	3.77	4.81
21.0	15.0	1.03	1.96	3.16	4.28	5.54
21.0	9.0	1.06	2.00	3.03	4.04	5.15
21.0	3.0	0.94	1.87	2.87	3.79	4.96

Table A2. NW Blower Duct Parameters at Five Blower Speeds

Controller Volts	Kurz (volts) average	Kurz (volt) std. dev.	Velocity (smps) average	Velocity (smps) std. dev.	Flow (scfm) Average	Flow (scfm) std. dev.
1	0.377	0.008	0.92	0.08	727.8	63.8
2	0.755	0.019	1.88	0.09	1479.9	71.9
3	1.199	0.017	2.89	0.15	2273.5	117.2
4	1.575	0.015	3.90	0.21	3068.3	169.1
5	2.014	0.019	5.07	0.26	3988.6	207.1

Table A3. NE Blower Duct Spatial Velocity at Five Blower Speeds

X (inch)	Y (inch)	Velocity (smps) 1 volt	Velocity (smps) 2 volt	Velocity (smps) 3 volt	Velocity (smps) 4 volt	Velocity (smps) 5 volt
3.0	21.0	0.81	1.71	2.66	3.62	4.58
3.0	15.0	0.87	1.96	3.05	4.22	5.39
3.0	9.0	0.81	2.04	3.14	4.21	5.43
3.0	3.0	0.75	1.72	2.56	3.62	4.62
9.0	21.0	0.87	1.77	2.71	3.66	4.65
9.0	15.0	0.86	1.95	2.93	3.99	5.05
9.0	9.0	0.80	2.04	3.09	4.24	5.39
9.0	3.0	0.63	1.84	2.90	4.01	5.05
15.0	21.0	0.83	1.71	2.62	3.55	4.50
15.0	15.0	0.86	1.82	2.78	3.75	4.80
15.0	9.0	0.81	1.97	3.02	4.03	5.14
15.0	3.0	0.62	1.73	2.86	3.88	4.93
21.0	21.0	0.78	1.63	2.55	3.45	4.37
21.0	15.0	0.87	1.87	2.83	3.79	4.78
21.0	9.0	0.85	1.88	2.92	3.88	4.90
21.0	3.0	0.67	1.70	2.55	3.51	4.49

Table A4. NE Blower Duct Parameters at Five Blower Speeds

Controller Volts	Kurz (volts) average	Kurz (volt) std. dev.	Velocity (smps) average	Velocity (smps) std. dev.	Flow (scfm) Average	Flow (scfm) std. dev.
1	0.349	0.004	0.79	0.06	623.9	50.8
2	0.811	0.006	1.83	0.11	1443.2	86.8
3	1.270	0.008	2.82	0.17	2222.5	131.7
4	1.657	0.011	3.84	0.22	3021.6	173.2
5	2.097	0.017	4.88	0.28	3842.5	222.6

Table A5. SW Blower Duct Spatial Velocity at Five Blower Speeds

X (inch)	Y (inch)	Velocity (smps) 1 volt	Velocity (smps) 2 volt	Velocity (smps) 3 volt	Velocity (smps) 4 volt	Velocity (smps) 5 volt
3.0	21.0	1.02	1.83	2.89	3.89	4.36
3.0	15.0	1.20	2.00	3.08	4.29	5.43
3.0	9.0	1.15	1.84	3.11	3.96	4.71
3.0	3.0	0.93	1.85	2.78	3.70	4.45
9.0	21.0	0.85	1.78	2.92	3.85	4.79
9.0	15.0	1.06	2.00	3.07	4.22	5.28
9.0	9.0	1.05	1.93	2.92	3.94	4.72
9.0	3.0	1.00	1.80	2.79	3.83	4.47
15.0	21.0	0.87	1.89	2.91	3.98	4.88
15.0	15.0	0.99	2.03	3.05	4.24	5.11
15.0	9.0	0.92	1.93	2.94	4.06	4.91
15.0	3.0	1.02	1.84	2.96	3.82	4.72
21.0	21.0	0.94	1.89	2.92	4.02	4.97
21.0	15.0	1.04	2.02	3.24	4.22	5.39
21.0	9.0	0.92	1.88	2.99	4.07	4.97
21.0	3.0	0.98	1.78	2.78	3.84	4.56

Table A6. SW Blower Duct Parameters at Five Blower Speeds

Controller Volts	Kurz (volts) average	Kurz (volt) std. dev.	Velocity (smps) average	Velocity (smps) std. dev.	Flow (scfm) Average	Flow (scfm) std. dev.
1	0.384	0.020	1.00	0.07	784.3	55.9
2	0.742	0.011	1.89	0.07	1490.0	55.1
3	1.199	0.017	2.96	0.10	2329.9	76.5
4	1.572	0.017	4.00	0.14	3146.4	113.8
5	1.934	0.026	4.86	0.26	3825.0	205.6

Table A7. E Blower Duct Spatial Velocity at Five Blower Speeds

X (inch)	Y (inch)	Velocity (smps) 1 volt	Velocity (smps) 2 volt	Velocity (smps) 3 volt	Velocity (smps) 4 volt	Velocity (smps) 5 volt
3.0	21.0	0.99	1.98	2.89	3.94	4.99
3.0	15.0	1.06	2.15	3.25	4.38	5.55
3.0	9.0	1.04	2.03	3.05	4.10	5.09
3.0	3.0	0.76	1.59	2.44	3.42	4.10
9.0	21.0	1.03	1.96	3.06	4.07	5.15
9.0	15.0	1.12	2.12	3.23	4.40	5.54
9.0	9.0	1.11	2.14	3.32	4.50	5.66
9.0	3.0	0.83	1.83	2.82	3.92	4.75
15.0	21.0	0.93	1.90	2.85	3.82	4.77
15.0	15.0	1.09	2.03	3.08	4.21	5.19
15.0	9.0	1.05	2.19	3.34	4.54	5.80
15.0	3.0	0.94	1.89	2.91	4.01	5.08
21.0	21.0	0.83	1.81	2.81	3.83	4.77
21.0	15.0	0.96	2.07	3.12	4.32	5.39
21.0	9.0	1.03	2.06	3.14	4.31	5.37
21.0	3.0	0.93	1.71	2.66	3.64	4.66

Table A8. SE Blower Duct Parameters at Five Blower Speeds

Controller Volts	Kurz (volts) average	Kurz (volt) std. dev.	Velocity (smps) average	Velocity (smps) std. dev.	Flow (scfm) Average	Flow (scfm) std. dev.
1	0.389	.010	0.98	0.09	772.7	67.7
2	0.778	.006	1.97	0.13	1548.2	106.1
3	1.214	.007	3.00	0.20	2361.8	157.5
4	1.595	.011	4.09	0.26	3218.7	202.1
5	1.979	.014	5.12	0.34	4029.4	267.6

APPENDIX B
Air Source Characterization Data

Table B1. Blower Flow Rate, Wind Speed & Direction for Panels at 600 SCFM

Panel	NE scfm		SE scfm		NW scfm		SW scfm		Wind Speed mph		Direction degrees	
	ave	S.D.	ave	S.D.	ave	S.D.	ave	S.D.	ave	S.D.	ave	S.D.
1	600	3	600	4	600	4	600	4	0	1	225	34
2	600	14	599	19	600	27	602	31	6	4	199	48
3	600	10	600	14	601	29	599	28	7	2	240	14
4	599	14	599	21	602	29	599	34	6	3	208	21
5	600	14	599	17	599	28	600	31	7	2	234	25
6	600	22	599	23	607	37	606	40	9	3	235	16
7	598	25	597	33	597	53	600	65	12	4	226	20
8	600	15	601	20	598	29	598	39	4	4	198	75
9	600	14	599	17	600	21	600	24	5	4	200	68
10	597	35	599	37	606	48	604	73	12	3	250	16
11	600	45	599	42	601	61	605	78	11	4	259	20
12	599	15	599	20	599	29	598	33	7	2	210	19
13	603	24	602	34	600	30	602	28	8	2	76	19
14	600	21	599	26	600	44	602	61	8	4	240	24
15	601	17	602	19	601	33	601	48	8	3	244	16
16	599	12	598	14	600	19	599	23	5	2	217	22
all	**600**	**19**	**600**	**22**	**600**	**33**	**601**	**42**	**7**	**4**	**220**	**47**

Table B2. Velocity Characterization Data for All Panels at 600 SCFM Blower Flows

panel	Vave (m/s)	Std. Dev. (m/s)	Std. Error
1	0.127	0.017	0.131
2	0.131	0.007	0.056
3	0.135	0.017	0.128
4	0.123	0.010	0.082
5	0.121	0.010	0.086
6	0.119	0.016	0.132
7	0.126	0.015	0.115
8	0.118	0.019	0.161
9	0.118	0.008	0.068
10	0.117	0.016	0.133
11	0.124	0.029	0.232
12	0.119	0.006	0.050
13	0.112	0.011	0.102
14	0.125	0.013	0.102
15	0.117	0.009	0.080
16	0.135	0.035	0.259
All panels	**0.123**	**0.018**	**0.145**

Table B3. Blower Flow Rate, Wind Speed & Direction for Panels at 1000 SCFM

Panel	NE scfm		SE scfm		NW scfm		SW scfm		Wind Speed mph		Direction degrees	
	ave	S.D.	ave	S.D.	ave	S.D.	ave	S.D.	ave	S.D.	ave	S.D.
1	1000	7	1001	8	999	16	1000	13	4	1	227	17
2	1000	13	1001	16	1000	35	1001	37	8	2	236	17
3	1000	8	1000	12	1001	17	1001	17	4	2	230	43
4	1000	10	999	14	999	22	1000	17	5	3	164	46
5	1001	13	1001	16	1002	33	1002	29	6	3	229	47
6	996	20	997	21	999	45	997	39	9	3	215	30
7	1000	20	999	28	999	62	999	56	13	4	224	16
8	999	15	998	21	1000	29	998	30	7	4	233	30
9	1002	23	1002	21	998	38	1003	46	10	3	256	17
10	999	25	999	22	998	43	1000	46	9	5	256	47
11	1000	42	999	31	1004	71	1002	65	11	3	263	19
12	1000	11	1000	16	1001	24	999	27	6	3	220	30
13	998	26	998	25	1000	16	999	21	6	2	92	25
14	999	20	998	24	997	49	999	52	11	3	252	21
15	1000	20	999	18	999	28	999	38	6	3	209	45
16	1000	10	1000	11	1000	21	999	19	5	3	224	33
all	**1000**	**18**	**999**	**19**	**1000**	**35**	**1000**	**36**	**7**	**4**	**223**	**46**

Table B4. Velocity Characterization Data for All Panels at 1000 SCFM Blower Flows

panel	Vave (m/s)	Std. Dev. (m/s)	Std. Error
1	0.192	0.042	0.218
2	0.205	0.014	0.071
3	0.206	0.026	0.125
4	0.182	0.019	0.102
5	0.184	0.017	0.094
6	0.174	0.034	0.195
7	0.189	0.022	0.114
8	0.179	0.030	0.170
9	0.177	0.015	0.086
10	0.168	0.027	0.160
11	0.178	0.035	0.197
12	0.178	0.012	0.068
13	0.163	0.022	0.134
14	0.187	0.019	0.099
15	0.168	0.017	0.102
16	0.220	0.147	0.671
All panels	**0.184**	**0.047**	**0.254**

Table B5. Blower Flow Rate, Wind Speed & Direction for Panels at 1500 SCFM

Panel	NE scfm		SE scfm		NW scfm		SW scfm		Wind Speed mph		Direction degrees	
	ave	S.D.	ave	S.D.	ave	S.D.	ave	S.D.	ave	S.D.	ave	S.D.
1	1500	8	1500	7	1500	14	1500	10	3	2	231	35
2	1500	15	1500	13	1501	27	1500	18	7	3	208	38
3	1501	8	1500	7	1500	6	1499	6	1	1	148	29
4	1500	14	1503	12	1500	30	1501	27	7	4	226	52
5	1500	13	1499	12	1496	24	1501	22	7	2	245	32
6	1501	19	1501	17	1500	48	1499	44	10	4	221	20
7	1500	22	1497	21	1499	43	1502	39	10	3	226	32
8	1499	17	1498	16	1499	41	1498	36	9	3	234	24
9	1500	17	1500	12	1499	38	1504	32	9	3	257	20
10	1498	30	1500	23	1499	52	1497	62	14	4	248	14
11	1504	45	1501	30	1504	68	1500	70	12	4	260	24
12	1499	15	1499	13	1499	32	1498	39	8	2	244	33
13	1505	27	1506	33	1500	13	1502	17	7	3	80	18
14	1500	21	1500	15	1504	46	1501	45	9	4	256	34
15	1499	15	1499	12	1501	30	1501	21	8	3	216	25
16	1500	13	1499	11	1500	36	1499	26	9	3	223	14
all	**1500**	**19**	**1500**	**16**	**1500**	**35**	**1500**	**34**	**8**	**4**	**220**	**50**

Table B6. Velocity Characterization Data for All Panels at 1500 SCFM Blower Flows

panel	Vave (m/s)	Std. Dev. (m/s)	Std. Error
1	0.278	0.073	0.263
2	0.296	0.024	0.081
3	0.299	0.033	0.111
4	0.265	0.032	0.121
5	0.267	0.030	0.111
6	0.251	0.044	0.176
7	0.270	0.032	0.117
8	0.260	0.044	0.168
9	0.248	0.028	0.113
10	0.244	0.042	0.170
11	0.254	0.038	0.151
12	0.257	0.020	0.079
13	0.239	0.035	0.145
14	0.270	0.030	0.110
15	0.238	0.025	0.104
16	0.295	0.108	0.367
All panels	**0.264**	**0.049**	**0.187**

Table B7. Blower Flow Rate, Wind Speed & Direction for Panels at 2000 SCFM

Panel	NE scfm		SE scfm		NW scfm		SW scfm		Wind Speed mph		Direction degrees	
	ave	S.D.	ave	S.D.	ave	S.D.	ave	S.D.	ave	S.D.	ave	S.D.
1	2000	10	2000	10	1999	24	2002	19	4	3	231	34
2	2000	9	2000	10	2000	25	2000	23	6	2	214	21
3	2000	8	2000	9	2000	8	2001	7	1	1	145	93
4	1998	18	1999	15	2000	36	1999	38	9	4	221	27
5	2000	15	1998	14	1996	37	1999	26	7	3	210	33
6	1999	19	1997	18	2003	43	1996	33	10	3	222	24
7	2000	16	1999	21	2003	53	1995	50	13	4	219	32
8	1999	11	1997	12	1998	45	2000	31	11	2	232	15
9	2001	17	2003	17	1998	56	1996	50	9	4	259	17
10	1998	19	2000	18	2006	75	2015	79	13	4	246	18
11	2000	32	2002	31	1995	90	2003	95	17	5	250	14
12	1999	16	1999	18	2000	39	2000	36	7	2	266	26
13	2001	36	2000	38	1997	19	1999	22	7	2	72	23
14	1999	19	2000	14	2002	59	2002	57	9	3	248	18
15	1999	10	2001	10	1999	40	1999	31	7	3	227	26
16	2001	11	1999	12	2000	42	2000	23	9	2	219	23
all	**2000**	**17**	**2000**	**17**	**2000**	**47**	**2001**	**45**	**8**	**5**	**220**	**55**

Table B8. Velocity Characterization Data for All Panels at 2000 SCFM Blower Flows

panel	Vave (m/s)	Std. Dev. (m/s)	Std. Error
1	0.353	0.103	0.293
2	0.380	0.039	0.104
3	0.379	0.042	0.111
4	0.351	0.031	0.089
5	0.341	0.041	0.121
6	0.321	0.048	0.149
7	0.347	0.043	0.123
8	0.332	0.064	0.193
9	0.318	0.039	0.121
10	0.309	0.069	0.224
11	0.325	0.045	0.137
12	0.330	0.029	0.087
13	0.307	0.051	0.165
14	0.348	0.053	0.152
15	0.302	0.034	0.114
16	0.369	0.119	0.323
All panels	**0.338**	**0.063**	**0.187**

Table B9. Blower Flow Rate, Wind Speed & Direction for Panels at 4000 SCFM

Panel	NE scfm		SE scfm		NW scfm		SW scfm		Wind Speed mph		Direction degrees	
	ave	S.D.	ave	S.D.	ave	S.D.	ave	S.D.	ave	S.D.	ave	S.D.
1	4000	10	4001	12	3998	32	4002	20	7	2	233	13
2	4002	10	4000	13	4001	24	3999	17	6	3	226	18
3	4000	12	4001	13	3998	11	3999	10	3	1	144	160
4	3999	12	4000	15	4009	45	4004	32	10	4	221	27
5	4000	13	4000	18	4001	27	3998	16	7	3	210	31
6	4000	11	4000	16	3995	54	4001	30	9	5	234	14
7	4001	11	3999	13	4000	44	4001	30	11	3	214	19
8	4000	11	3998	11	4000	33	3999	26	6	3	228	31
9	4000	15	4000	15	3999	50	3999	40	9	3	264	20
10	4000	16	3997	19	3989	61	4002	47	11	3	274	33
11	3999	26	4003	32	4002	129	4004	111	23	6	250	16
12	4001	15	4000	18	3997	51	4000	40	9	2	268	16
13	3998	11	3999	18	4000	13	3999	14	2	2	206	114
14	4000	15	4000	16	4002	58	4000	44	9	4	267	20
15	3998	12	3999	16	4003	44	4000	29	9	2	233	15
16	3999	13	4002	15	4002	38	4000	23	8	3	220	19
all	**4000**	**14**	**4000**	**17**	**4000**	**54**	**4000**	**43**	**9**	**6**	**231**	**64**

Table B10. Velocity Characterization Data for All Panels at 4000 SCFM Blower Flows

panel	Vave (m/s)	Std. Dev. (m/s)	Std. Error
1	0.725	0.220	0.303
2	0.761	0.097	0.127
3	0.758	0.110	0.146
4	0.716	0.090	0.126
5	0.702	0.131	0.187
6	0.662	0.095	0.144
7	0.721	0.124	0.172
8	0.690	0.154	0.224
9	0.650	0.117	0.180
10	0.641	0.171	0.266
11	0.663	0.094	0.142
12	0.679	0.082	0.121
13	0.627	0.112	0.178
14	0.708	0.111	0.157
15	0.619	0.119	0.192
16	0.753	0.314	0.417
All panels	**0.692**	**0.152**	**0.219**

DISTRIBUTION

E. J. Weckman
Mechanical Engineering Department
University of Waterloo
Waterloo, Ontario, Canada N2L 3G1

Rod W. Oliver
1661 Braudview
Jenison, MI 49428

MS0736 T. E. Blejwas, 6400
MS1139 K. O. Reil, 6423
MS1139 J. H. Bentz, 6423
MS1139 T. E. Blanchat, 6423 (10)
MS1139 C. R. Hanks, 6423
MS1139 J. Garcia, 6423
MS0841 T. C. Bickel, 9100
MS0834 T Y Chu, 9100 (2)
MS0824 A. C. Ratzel, 9112
MS0834 S. P. Kearney, 9112
MS0834 P. Drozda, 9112
MS0834 T. J. O'Hern 9112 (3)
MS0836 E. S. Hertel, 9116
MS0553 W. Gill, 9116 (2)
MS0836 C. E. Hickox, 9116
MS0836 V. F. Nicolette, 9116
MS0836 S. R. Tiezsen, 9116 (3)
MS0836 J. M. Suo-Anttila, 9116
MS0824 J. L. Moya, 9132
MS0828 M. Pilch, 9133
MS0828 B. F. Blackwell, 9133
MS0828 A. R. Lopez, 9133
MS0555 J. T. Nakos, 9134
MS0555 M. O. Ramirez, 9134
MS0405 K. B. Sobolik, 12333
MS0839 L. A. Gritzo, 16000
MS9018 Central Technical Files (8945-1)
MS0899 Technical Library, 9616 (2)
MS0612 Review and Approval Desk, 9612
For DOE/OSTI